

UNIVERSITÉ DU QUÉBEC À MONTRÉAL

GENERALIZATION OF CATALAN COMBINATORICS TO THE CONTEXT OF
GRAPHS

THESIS

PRESENTED

IN PARTIAL FULFILLMENT

OF THE MASTER'S DEGREE IN MATHEMATICS

BY

MARJAN RASHTCHI

JANUARY 2016

UNIVERSITÉ DU QUÉBEC À MONTRÉAL
Service des bibliothèques

Avertissement

La diffusion de ce mémoire se fait dans le respect des droits de son auteur, qui a signé le formulaire *Autorisation de reproduire et de diffuser un travail de recherche de cycles supérieurs* (SDU-522 – Rév.07-2011). Cette autorisation stipule que «conformément à l'article 11 du Règlement no 8 des études de cycles supérieurs, [l'auteur] concède à l'Université du Québec à Montréal une licence non exclusive d'utilisation et de publication de la totalité ou d'une partie importante de [son] travail de recherche pour des fins pédagogiques et non commerciales. Plus précisément, [l'auteur] autorise l'Université du Québec à Montréal à reproduire, diffuser, prêter, distribuer ou vendre des copies de [son] travail de recherche à des fins non commerciales sur quelque support que ce soit, y compris l'Internet. Cette licence et cette autorisation n'entraînent pas une renonciation de [la] part [de l'auteur] à [ses] droits moraux ni à [ses] droits de propriété intellectuelle. Sauf entente contraire, [l'auteur] conserve la liberté de diffuser et de commercialiser ou non ce travail dont [il] possède un exemplaire.»

UNIVERSITÉ DU QUÉBEC À MONTRÉAL

GÉNÉRALISATION DE LA COMBINATOIRE DE CATALAN AU CONTEXTE
DES GRAPHS

MÉMOIRE
PRÉSENTÉE
COMME EXIGENCE PARTIELLE
DE LA MAÎTRISE EN MATHÉMATIQUES

PAR
MARJAN RASHTCHI

JANVIER 2016

ACKNOWLEDGEMENT

Firstly, I would like to express my sincere gratitude to my supervisor, Prof. François Bergeron for the continuous support of my Master study and related research, for his patience, motivation, and immense knowledge. His guidance helped me in all the time of research and writing of this thesis. I could not have imagined having a better advisor and mentor for my Master study.

I am also very grateful to my program's director Dr. Olivier Collin who helped me a lot through my study.

I must acknowledge as well all the professors and friends at LaCIM who inspired and supported me and my efforts over these years. Particularly, I need to express my gratitude and deep appreciation to Jose Eduardo Blazek, Alejandro Morales, Amy Pang, and Yannic Vargas Lozada.

Last but not the least, I would like to thank my parents who not only tolerated my absence, but also supported me while I was away from home, and to my brother for supporting me throughout writing this thesis. Also, I would like to especially thank my husband, who is always there cheering me up and stands by me through the good times and bad.

CONTENTS

LIST OF TABLES	ix
LIST OF FIGURES	xi
RÉSUMÉ	xv
ABSTRACT	xvii
INTRODUCTION	1
CHAPTER I	
SOME BACKGROUND IN COMBINATORICS	3
1.1 Graphs	3
1.2 Posets	5
1.2.1 Zeta polynomials	7
1.2.2 Lattices	9
1.3 Catalan numbers	10
1.4 Symmetric group S_n	10
CHAPTER II	
SOME CATALAN OBJECTS	13
2.1 Binary trees	13
2.2 Complete binary trees	14
2.3 Dyck paths	14
2.3.1 Count the number of Dyck paths	15
2.4 Dyck words	16
2.5 Bijection between complete binary trees and Dyck paths	17
2.6 Bounded increasing sequences	19
CHAPTER III	
TAMARI POSET ON CATALAN OBJECTS	23
3.1 Tamari poset	23
3.2 Tamari poset on binary trees	25
3.3 Tamari poset on Dyck paths	27
3.4 Tamari poset on Dyck words	28
CHAPTER IV	
PARKING FUNCTIONS ON CATALAN OBJECTS	31

4.1	Parking functions	31
4.1.1	Count the number of parking functions	34
4.2	Parking functions on Dyck paths	34
4.2.1	Labeled intervals	36
4.3	Parking functions on Dyck words	39
4.4	Parking functions on complete binary trees	40
4.5	Zeta polynomial for parking functions enumeration	41
CHAPTER V		
COMBINATORICS OF TUBINGS		
5.1	Tubings of graphs	45
5.2	Path graphs give Catalan objects	48
5.2.1	Bijection between maximal tubings of path graph and binary trees	48
5.2.2	Tamari order on maximal tubings of path graphs	50
5.2.3	Parking functions on maximal tubings of path graphs	52
5.3	Maximal tubings of other special families of graphs	53
5.3.1	Complete graphs	53
5.3.2	Discrete graphs	54
5.3.3	Cycle graphs	55
5.3.4	Star graphs	55
5.4	Toward a new generalization of parking functions to graphs	56
CONCLUSION		57
BIBLIOGRAPHY		59

LIST OF TABLES

Tableau	Page
3.1 Some values of the zeta polynomials for the Tamari posets $\mathcal{T}_1, \mathcal{T}_2, \mathcal{T}_3$, and \mathcal{T}_4	25
5.1 Some values of maximal tubings and compatible labelings of maximal tubings for cycle graphs.	58
5.2 Some values of maximal tubings and compatible labelings of maximal tubings for star graphs.	58

LIST OF FIGURES

Figure	Page
1.1 A graph.	3
1.2 Illustration of a subgraph (left) and an induced subgraph (right) of a graph.	4
1.3 A graph with three connected components.	5
1.4 The poset of subsets of $\{1, 2, 3\}$ under inclusion.	6
1.5 A path, complete, and cycle graphs in terms of poset.	6
1.6 Poset P	8
1.7 Weak order on \mathbb{S}_3	11
2.1 The set B_3 , of binary trees with 3 nodes.	13
2.2 The set C_3 , of complete binary trees with 7 nodes.	14
2.3 The set D_3 , of Dyck paths of size 3.	14
2.4 A Dyck path with composition 21	15
2.5 Non-Dyck path (in red), and its reflected part (in black).	15
2.6 The post-order of this tree is $e, f, g, d, h, c, b, i, a$	17
2.7 Transforming the complete binary tree to Dyck path.	17
2.8 Dyck path which meets the diagonal (left one), and does not meet the diagonal (right one). 18	
2.9 Transforming the Dyck path $SESE$ to a complete binary tree.	18
2.10 General form of transforming Dyck path SME to a complete binary tree.	19
2.11 Transforming the Dyck path $SSESESE$ to a complete binary tree.	19
2.12 Sequence $(1, 1, 1, 3) \rightarrow$ Dyck path $SSSESESE$	20
2.13 Dyck path $SSESESE$ \rightarrow sequence $(1, 1, 3, 4)$	20
3.1 The Tamari lattice \mathcal{T}_3	24
3.2 The enumeration of intervals in Tamari lattice \mathcal{T}_3	24
3.3 Right-rotation.	25
3.4 Notion of $t_1 \prec t_2$	26

3.5	The Tamari lattice of complete binary trees for $n = 3$ (left) and $n = 4$ (right).	26
3.6	The Tamari lattice of binary trees for $n = 3$ (left) and $n = 4$ (right).	27
3.7	Notion of $d_1 \prec d_2$.	27
3.8	The Tamari lattice of Dyck paths for $n = 3$ (left) and $n = 4$ (right).	28
3.9	Two triangulations T and T' are being related by an edge flip.	29
4.1	211 is a parking function of length 3.	32
4.2	Define function f on the set of labels.	34
4.3	Parking functions over one Dyck path of size 3.	35
4.4	Enumeration of Dyck paths with $(r_1 = 1, r_2 = 1, r_3 = 0)$.	36
4.5	How σ permutes the labels of a labeled Dyck path of D_4 .	37
4.6	Stable labeled Dyck paths of D_3 by σ .	37
4.7		38
4.8	Parking functions over a complete binary tree of C_3 .	40
4.9	Parking functions over one complete binary tree of size 3.	41
4.10	The Tamari poset \mathcal{T}_3 with the associated bounded increasing sequences.	42
5.1	Valid tubings of some connected graphs.	46
5.2	Invalid tubings of some connected graphs.	46
5.3	Valid tubings of some graphs with several connected components.	46
5.4	Invalid tubings of some graphs with several connected components.	46
5.5	Poset of tubings of a path graph with 3 nodes.	47
5.6	Representation of function f .	48
5.7	Transforming a maximal tubing of a path graph to the corresponding binary tree.	49
5.8	Transforming a binary tree to the corresponding maximal tubing of a path graph.	50
5.9	Notion of $U_1 \prec U_2$.	50
5.10	The Tamari lattice that results from maximal tubings on the path graph for $n=3$ (left) and $n=4$ (right).	51
5.11	Pushing the tubes in order from smallest one, right to left.	51
5.12	A compatible labeling for a path graph with five vertices.	52
5.13	Parking functions on the maximal tubing of a 3-path graph.	53

5.14 A covering relation in the weak order on permutations.	54
5.15 The lattice that results from maximal tubings on the complete graph with 3 vertices. . . .	54
5.16 The lattice that results from maximal tubings on the three disjoint nodes.	55
5.17 The lattice that results from maximal tubings on the star graph S_2	56
5.18 A compatible labeling for a cycle graph with three vertices.	56
5.19 Parking functions on maximal tubings of the complete graph with three vertices.	57

RÉSUMÉ

Il est question dans le présent document de certaines familles d'objets mathématiques dont la cardinalité se dénombre par la célèbre suite des nombres de Catalan. Nous nous concentrons sur certaines propriétés du treillis de Tamari. Nous considérons aussi les relations entre ces objets et les fonctions de stationnement. Afin d'étendre ces constructions à d'autres contextes, nous introduisons la notion de « tube de graphe ». Pour les graphes de chemins, ceci retrouve la configuration de Catalan. Par cette analogie, nous pouvons généraliser à d'autres familles de graphes tels que les graphes complets, cycliques, etc.

Mots-clés: Nombre de Catalan, objets de Catalan, treillies de Tamari, polynôme de zeta, fonctions de stationnement, tube de graphe.

ABSTRACT

In the present document we investigate families of mathematical objects counted by the famous sequence of Catalan numbers. We are interested in properties of some structures on such families known as the Tamari lattices. We consider relations between those objects and parking functions. To extend such constructions to other contexts, we introduce the notion of "graph tubing". For path graphs, this recovers the Catalan setup. Using this analogy, we can generalize the theory to other nice families of graphs such as complete graphs, cycle graphs, etc.

Keywords: Catalan numbers, Catalan objects, Tamari lattice, zeta polynomials, parking functions, graph tubing.

INTRODUCTION

Catalan numbers have always been considered as an important integer sequence in combinatorics with several characterizations, and there are several interesting families of mathematical objects counted by these numbers, which are named Catalan objects. On the other hand, Dov Tamari in [15, 1962] introduced a lattice structure on the family of well-formed parentheses whose number of elements is the Catalan number. There are some interesting results on the Tamari lattice such as Chapoton's formula to count the number of intervals in this lattice. Furthermore, there are other combinatorial notions such as Parking functions, whose connections to Catalan objects are interesting. Any time a new family emerges whose elements are enumerated by the Catalan numbers, we are motivated to find the associated Tamari order on its poset.

In [5, 2005] M. Carr and S. Devadoss introduced the notion of "graph tubing" in which, specially for path graphs, the number of maximal tubings is the Catalan number. Hence maximal tubings of a path graph is yet another class of Catalan objects. In [11, 2012] M. Ronco described a partial order on the set of tubings of a simple graph, which generalized the Tamari order on the set of tubings of path graphs. During the same year, S. Forcey in [8] generalized the Tamari order, and the weak order on permutations, to maximal tubings of a graph.

In the present work, our goal is to relate parking functions to maximal tubings of path graphs as a recent Catalan object. This opens the possibility of considering parking functions for maximal tubings of other "nice" families of graphs, such as complete graphs, cycle graphs, etc.

The first chapter of this monograph recalls some basic combinatorial notions namely: posets, intervals in posets, lattices, the zeta polynomial, Catalan numbers, and the symmetric group \mathbb{S}_n . In the second chapter, we introduce some of the Catalan objects such as Dyck paths, Dyck words, binary trees, and complete binary trees. Although there are direct individual proofs that the cardinality of Dyck paths, binary trees or other Catalan families are indeed given by Catalan numbers, we will rather prove this for just one case (Dyck paths), and then show that there are bijections linking other families to this specific one. In Chapter 3, we translate the Tamari lattice structure to the context of the considered families, and interpret the order directly in the relevant context. In Chapter 4, the properties of parking functions are discussed, and we consider how parking functions may be defined directly in each context. Also we extend the enumeration of parking functions using zeta polynomials. We start Chapter 5 with the definition of tubing and its properties, and also we recall how to count the number of maximal tubings for some

special families of graphs, such as path graphs, complete graphs, and cycle graphs. We describe the Tamari order defined by Forcey, and continue with the spirit of parking functions in terms of maximal tubings of path graphs.

CHAPTER I

SOME BACKGROUND IN COMBINATORICS

In this chapter we introduce some combinatorial terminology such as graphs, posets, intervals in posets, lattices, zeta polynomials, Catalan numbers, and symmetric groups \mathbb{S}_n which will be used later .

1.1 Graphs

A (simple) *graph* is a pair of sets, denoted $G = (V, E)$, where V is a finite set and E is a subset of $\binom{V}{2}$, which stands for the set of pairs of elements in V . The set V is called the set of *vertices* (or nodes), and E is called the set of *edges* of G . The edge $e = \{u, v\} \subseteq \binom{V}{2}$ is also denoted by $e = uv$, and then u is said to be *adjacent* to v , and u is said to be *incident* to e . If the edges of G are directed, then the graph is called an *oriented graph*, and the edges are called *arcs*. For example, Figure 1.1 represents a graph with set of vertices $V = \{v_1, v_2, v_3, v_4, v_5\}$ and set of edges $E = \{v_1v_2, v_2v_3, v_3v_4, v_4v_5, v_1v_5, v_2v_5\}$.

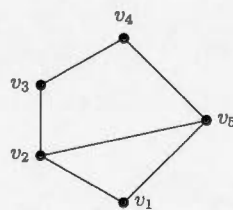


Figure 1.1: A graph.

What happens in the structure of a graph is satisfying the following function:

$$\mathbb{S}_V \times \text{Graphs}[V] \rightarrow \text{Graphs}[V]$$

$$\sigma, G \mapsto \sigma \cdot G := (V, \sigma \cdot E)$$

such that:

- $\mathbb{S}_V := \{\sigma \mid \sigma : V \rightarrow V\}$. (see Section 1.4)
- $\text{Graphs}[V] := \{(V, E) \mid E \subseteq \binom{V}{2}\}$.
- $\sigma \cdot E := \{\{\sigma(u), \sigma(v)\} \mid \{u, v\} \in E\}$.

Then two graphs G_1 and G_2 are *isomorphic* if and only if there exists a function σ in \mathbb{S}_V such that $\sigma \cdot G_1 = G_2$, denoted $G_1 \sim G_2$. This is an equivalence relation. Hence a graph type (shape) is an equivalence class for this isomorphism relation

$$[G] \in \text{Graphs}[V]/\sim.$$

We will informally refer to an equivalence class $[G]$ as an *unlabeled* graph. Indeed, it is customary to draw unlabeled graphs with undistinguishable vertices (simple dots).

A *subgraph* of G , is a graph whose vertices are a subset of the vertex set of G , and whose edges are a subset of the edge set of G . A subgraph, G_1 of G , is *induced*, if for any pair of vertices u and v of G_1 , uv is an edge of G_1 if and only if uv is an edge of G . For example, Figure 1.2 shows a subgraph, and induced subgraph on the red vertices of a given graph.

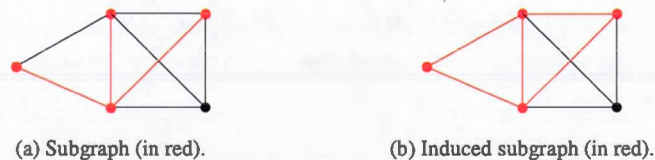


Figure 1.2: Illustration of a subgraph (left) and an induced subgraph (right) of a graph.

A graph is *connected*, if there is a path between each pair of the vertices. Otherwise, the graph is disconnected and its largest connected subgraphs are called *connected components* of graph. For example, Figure 1.3 shows a graph with three connected components.

In the following we mostly consider some special families of graphs, such as:

- *Path graphs*: a graph with vertex set $V = \{v_1, \dots, v_n\}$ such that the set of edges is

$$\{\{v_i, v_{i+1}\} \mid 1 \leq i \leq n - 1\}.$$

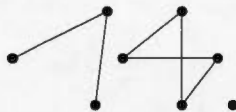


Figure 1.3: A graph with three connected components.

- *Complete graphs*: a graph with all possible edges.
- *Cycle graphs*: a path graph with extra edge $\{v_1, v_n\}$ between the first and last vertices.

1.2 Posets

Let us now recall some background from the theory of posets, which plays an important role in enumerative combinatorics. An excellent reference for general theory of posets is [12, Chapter 3]. A *partially ordered set* P , or poset for short, is a set P together with a binary relation " \preceq ", satisfying the following relations:

- For all $x \in P$, $x \preceq x$. (reflexivity)
- If $x \preceq y$, and $y \preceq x$, then $x = y$. (antisymmetry)
- If $x \preceq y$, and $y \preceq z$, then $x \preceq z$. (transitivity)

Two elements $x, y \in P$ are *comparable* if $x \preceq y$ or $y \preceq x$, otherwise x and y are *incomparable*. An element x of a poset is called *maximal* if for all element $y \in P$, $x \not\preceq y$, and x is *minimal* if for all element $y \in P$, $y \not\preceq x$. If maximal and minimal elements are unique in the poset, are called respectively maximum and minimum, denoted $\hat{1}, \hat{0}$. A *chain* in a poset is a subset $C \subseteq P$ such that any two elements in C are comparable, and it is called *multi-chain* if it has repeated elements. A chain with n elements is a chain of length $n - 1$. Let x and y be two distinct elements of a poset P . We say that y *covers* x or x is covered by y , denoted $x \prec y$, if $x \preceq y$ (i.e., $x \preceq y$ and $x \neq y$) and no element z satisfies $x \prec z \prec y$. A finite poset is determined by a *Hasse diagram*; this is the oriented graph whose vertices are the elements of the poset, and whose arcs correspond to the covering relations such that, if $x \prec y$ then y is drawn above x . So the Hasse diagram is directed in the plane from bottom to top.

For example, Figure 1.4 is the Hasse diagram of the poset of subsets of $\{1, 2, 3\}$. The order relation in this poset is set inclusion: $x \preceq y$ if $x \subseteq y$. The minimum element is $\{\}$, and the maximum element is $\{1, 2, 3\}$. For instance, $\{\} \preceq \{3\} \preceq \{2, 3\}$ is a chain with three elements such that $\{2, 3\}$ covers $\{3\}$ but it does not cover $\{\}$.

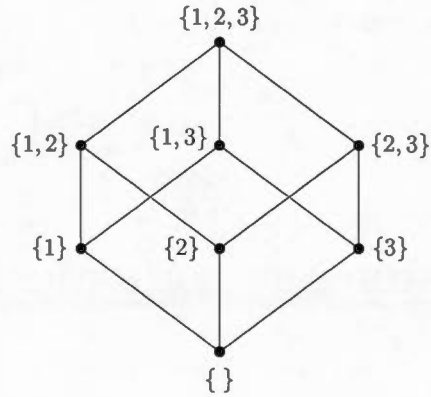


Figure 1.4: The poset of subsets of $\{1, 2, 3\}$ under inclusion.

For a partially ordered set (P, \preceq) , let $x, y \in P$ with $x \preceq y$. The set $[x, y] = \{z \in P \mid x \preceq z \preceq y\}$ is called an *interval* of P . The cardinality of $[x, y]$ is the number of multi-chains between x and y with three elements. For example, in the poset Figure 1.4, $[\{\}, \{2, 3\}] = \{\{\}, \{2\}, \{3\}, \{2, 3\}\}$ is an interval with four elements. Hence we have four following multi-chains between $\{\}$ and $\{2, 3\}$:

$$\begin{aligned} \{\} &\preceq \{\} \preceq \{2, 3\} \\ \{\} &\preceq \{3\} \preceq \{2, 3\} \\ \{\} &\preceq \{2\} \preceq \{2, 3\} \\ \{\} &\preceq \{2, 3\} \preceq \{2, 3\}. \end{aligned}$$

In the section 1.1, we introduced path, complete, and cycle graphs as a special families of graphs, therefore it would be interesting to consider them as a poset and study the number of multi-chains with three elements between minimum and maximum elements of the poset.

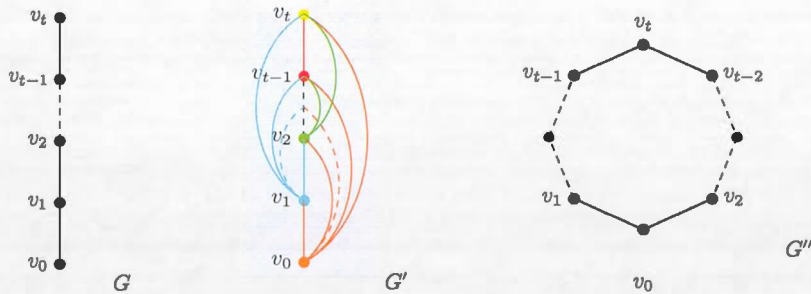


Figure 1.5: A path, complete, and cycle graphs in terms of poset.

Figure 1.5 illustrates a path graph G , a complete graph G' , and cycle graph G'' as a poset with $t + 1$ elements on vertex set $\{v_0, v_1, \dots, v_t\}$ where $v_0 = \hat{0}$ is the minimum element, and $v_t = \hat{1}$ is the maximum element. The cardinality of $[\hat{0}, \hat{1}]$ in every mentioned poset is:

$$[\hat{0}, \hat{1}]_G = \{v_0, v_1, v_2, \dots, v_{t-1}, v_t\} \quad ; \quad |[\hat{0}, \hat{1}]_G| = t + 1.$$

$$[\hat{0}, \hat{1}]_{G'} = \{v_0, v_1, v_2, \dots, v_{t-1}, v_t\} \quad ; \quad |[\hat{0}, \hat{1}]_{G'}| = t + 1.$$

$$[\hat{0}, \hat{1}]_{G''} = \{v_0, v_1, v_2, \dots, v_{t-2}, v_{t-1}, v_t\} \quad ; \quad |[\hat{0}, \hat{1}]_{G''}| = t + 1.$$

There are $t + 1$ multi-chains with three elements in each poset G, G' , and G'' :

$$\left\{ \begin{array}{l} v_0 \preceq v_0 \preceq v_t \\ v_0 \preceq v_1 \preceq v_t \\ v_0 \preceq v_2 \preceq v_t \\ \vdots \\ v_0 \preceq v_{t-1} \preceq v_t \\ v_0 \preceq v_t \preceq v_t \end{array} \right.$$

Similarly, for other vertices of G and G' we have:

$$|[\hat{0}, v_{t-1}]_G| = |[\hat{0}, v_{t-1}]_{G'}| = t.$$

$$|[\hat{0}, v_{t-2}]_G| = |[\hat{0}, v_{t-2}]_{G'}| = t - 1.$$

\vdots

$$|[\hat{0}, v_1]_G| = |[\hat{0}, v_1]_{G'}| = 2.$$

$$|[\hat{0}, v_0]_G| = |[\hat{0}, v_0]_{G'}| = 1.$$

Hence the number of intervals in the posets G and G' is

$$\sum_{k=1}^{t+1} k = \frac{(t+1)(t+2)}{2}.$$

To find the number of intervals in poset G'' , it suffices to consider poset G'' as a join of two left and right path posets such that the left one has t_l vertices, and the right one has t_r vertices (except v_0 and v_t). Then count the number of intervals for each path poset such as what we did for poset G . Hence the number of intervals in poset G'' is

$$(t+1) + \sum_{k=2}^{t_l+1} k + \sum_{k=2}^{t_r+1} k + 1.$$

1.2.1 Zeta polynomials

One of the subjects that has useful results on posets is the zeta polynomial. First we define some related constants. For a poset (P, \preceq) , suppose $x, y \in P$, then let $\mathcal{D}_P^n(x, y)$ be the set of sequences called (weak)

chain defined as follows:

$$\mathcal{D}_P^n(x, y) := \{(x_0, \dots, x_n) \mid x = x_0 \prec x_1 \prec \dots \prec x_n = y\}.$$

and let $\mathcal{C}_P^n(x, y)$ be the set of sequences called multi-chains defined as follows:

$$\mathcal{C}_P^n(x, y) := \{(x_0, \dots, x_n) \mid x = x_0 \preceq x_1 \preceq \dots \preceq x_n = y\}.$$

The *zeta polynomial*, $Z_P(n)$, for a poset P with minimal and maximal elements $\hat{0}, \hat{1}$ respectively, is defined as follows:

$$Z_P(n) := |\mathcal{C}_P^n(\hat{0}, \hat{1})|.$$

As a polynomial in n , we have (see [12]):

$$Z_P(n) = \sum_{k \geq 0} \binom{n}{k} |\mathcal{D}_P^k(\hat{0}, \hat{1})|. \quad (1.2.1)$$

For example, for the poset P in Figure 1.6 with minimum element a and maximum element e , the zeta polynomial is:

$$Z_P(n) = \frac{1}{6}(n^3 + 6n^2 - n).$$

One gets the following binomial coefficient expansion:

$$Z_P(n) = n + 3 \binom{n}{2} + \binom{n}{3}.$$

This is so since:

$$\begin{aligned} Z_P(n) &= \binom{n}{1} |\{(a, e)\}| \\ &\quad + \binom{n}{2} |\{(a, b, e), (a, c, e), (a, d, e)\}| \\ &\quad + \binom{n}{3} |\{(a, b, c, e)\}|. \end{aligned}$$

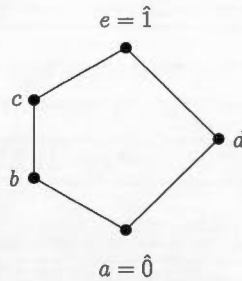


Figure 1.6: Poset P .

As a result, we have $Z_P(2) = 5$, so it means that the multi-chains with three elements count the elements of poset P , and $Z_P(3) = 13$ which means that the multi-chains with four elements count the intervals of

the poset.

We can also calculate the zeta polynomial for posets of a path graph, a complete graph, and a cycle graph of Figure 1.5 with $n + 1$ vertices:

$$Z_G(n) = n + (t-1) \binom{n}{2} + (t-2)! \binom{n}{3} + (t-3)! \binom{n}{4} + \dots$$

This is so since:

$$\begin{aligned} Z_G(n) &= \binom{n}{1} |\{(v_0, v_t)\}| \\ &+ \binom{n}{2} |\{(v_0, v_1, v_t), (v_0, v_2, v_t), \dots, (v_0, v_{t-1}, v_t)\}| \\ &+ \binom{n}{3} |\{(v_0, v_1, v_2, v_t), (v_0, v_1, v_3, v_t), \dots, (v_0, v_1, v_{t-1}, v_t) \\ &\quad (v_0, v_2, v_3, v_t), (v_0, v_2, v_4, v_t), \dots, (v_0, v_2, v_{t-1}, v_t) \\ &\quad \vdots \\ &\quad (v_0, v_{t-2}, v_{t-1}, v_t)\}| \\ &+ \dots \end{aligned}$$

The $Z_{G'}(n)$ is the same as the $Z_G(n)$. For calculate $Z_{G''}(n)$, G'' as a join of two paths that the left one contains t_l vertices, and the right path contains t_r vertices (except v_0 and v_1), we have the following polynomial:

$$Z_{G''}(n) = n + (t-1) \binom{n}{2} + ((t_l-1)! \binom{n}{3} + (t_l-2)! \binom{n}{4} + \dots) + ((t_r-1)! \binom{n}{3} + (t_r-2)! \binom{n}{4} + \dots)$$

1.2.2 Lattices

An important class of posets is known as lattices. To introduce lattices, first recall some definitions. Let (P, \preceq) be a partially ordered set. An *upper bound* of $x, y \in P$ is an element $z \in P$ satisfying $x \preceq z$ and $y \preceq z$. A least upper bound of x and y is an upper bound z such that every upper bound z' of x and y satisfies $z \preceq z'$. A least upper bound of x and y is unique if it exists, and is called their *join*, denoted $x \vee y$. Similarly, a *lower bound* of $x, y \in P$ is an element $z \in P$ satisfying $z \preceq x$ and $z \preceq y$. A greatest lower bound of x and y is a lower bound z such that every lower bound z' of x and y satisfies $z' \preceq z$. A greatest lower bound of x and y is unique if it exists, and is called their *meet*, denoted $x \wedge y$.

A *lattice* is a poset for which every pair of elements has a join and meet. A lattice as an algebraic structure in terms of the operations \vee and \wedge , satisfies the following axioms:

- Commutative law: $x \vee y = y \vee x$, $x \wedge y = y \wedge x$.
- Associative law: $x \vee (y \vee z) = (x \vee y) \vee z$, $x \wedge (y \wedge z) = (x \wedge y) \wedge z$.
- Absorption law: $x \wedge (x \vee y) = x = x \vee (x \wedge y)$.

- Idempotent law: $x \vee x = x \wedge x = x$.
- $x \wedge y = x \Leftrightarrow x \vee y = y \Leftrightarrow x \preceq y$.

For example, the poset in Figure 1.4 is a lattice that $\{1\} \vee \{3\} = \{1, 3\}$, and $\{1\} \wedge \{3\} = \{\}$.

1.3 Catalan numbers

As illustrated by a famous exercise in Stanley's book [13], one of the best known integer sequences in combinatorics is the sequence of Catalan numbers. *Catalan numbers* are defined by

$$C(n) = \frac{1}{n+1} \binom{2n}{n}. \quad (1.3.1)$$

In 1838, Belgian mathematician Eugène Charles Catalan was the first to obtain what is now a standard formula for Catalan numbers. Small values of $C(n)$ are:

$$1, 1, 2, 5, 14, 42, 132, 429, 1430, \dots$$

The Catalan numbers satisfy the following recurrence relation for $n > 0$ where $C(0) = 1$,

$$C(n+1) = \sum_{k=0}^n C(k)C(n-k). \quad (1.3.2)$$

As is frequently useful in combinatorics, we can try to calculate or get a formula for $C(n)$ by using a generating function. This means that for a power series $B(x)$ defined by

$$B(x) := \sum_n C(n)x^n,$$

in terms of the generating function, we have

$$B(x) = 1 + xB(x)^2,$$

which is simply a translation of the recursive definition of Catalan number (for more details see [3]).

We will have many families of objects (grouped by "size"), such that the number of those objects in size n is equal to $C(n)$. For this reason, we will say that such objects are "Catalan objects". This will be the subject of the next chapter.

1.4 Symmetric group \mathbb{S}_n

The *symmetric group* \mathbb{S}_n is the group of bijections of $[n] = \{1, \dots, n\}$ to itself. The cardinality of this set is equal to $n!$. A notation for the permutation that sends $i \rightarrow l_i$ is

$$\sigma = l_1 l_2 \dots l_n.$$

A k -cycle permutation (or a cycle of length k) is a permutation that sends l_i to l_{i+1} for $1 \leq i \leq k - 1$ and l_k to l_1 , denoted

$$(l_1 l_2 \dots l_k).$$

The same cycle can be written in several ways, by cyclically permuting the l_j . For example, it also can be written as:

$$(l_2 l_3 \dots l_k l_1) \text{ or } (l_3 l_4 \dots l_k l_1 l_2).$$

Two cycles $(l_1 l_2 \dots l_k)$ and $(l'_1 l'_2 \dots l'_{k'})$ are *disjoint*, when the sets $\{l_1, \dots, l_k\}$ and $\{l'_1, \dots, l'_{k'}\}$ are disjoint. Every permutation $\sigma \in \mathbb{S}_n$ is expressible as a product of disjoint cycles uniquely, which is called the *cycle decomposition* of σ . For example, $\sigma = 25431$ in \mathbb{S}_5 has a cycle decomposition $(2\ 5\ 1)(3\ 4)$.

Let $\bigcup_{i=1}^k n_i = \{1, 2, \dots, n\}$ be a partition of $\{1, 2, \dots, n\}$ into k disjoint subsets. Then the corresponding *Young subgroup* of \mathbb{S}_n , is the subgroup

$$\mathbb{S}_{n_1} \times \mathbb{S}_{n_2} \times \dots \times \mathbb{S}_{n_k},$$

where $\mathbb{S}_{n_i} = \{\sigma \in \mathbb{S}_n : \sigma(j) = j \text{ for all } j \notin n_i\}$, that consists of $|n_i|!$ of such σ . This means that σ permutes the elements of n_i , and fixes the elements in the complement $\{1, 2, \dots, n\} \setminus n_i$.

For a permutation σ in \mathbb{S}_n , an *inversion* set of σ , denoted $\text{Inv}(\sigma)$, is the set of pairs (i, j) with $i < j$ and $l_i > l_j$. For example, $\text{Inv}(\sigma = 312) = \{(1, 2), (1, 3)\}$, because $l_1 = 3 > l_2 = 1$ and $l_1 = 3 > l_3 = 2$.

The *weak order* on the symmetric group is a partial order such that for $\sigma, \theta \in \mathbb{S}_n$, $\sigma \preceq \theta$ whenever $\text{Inv}(\sigma) \subseteq \text{Inv}(\theta)$. This poset is a lattice with identity permutation, $123\dots n$ as the minimum element, and the permutation formed by reversing the identity, $n\ n - 1\dots 321$ as the maximum element. The covering relation $\sigma \prec \theta$ occurs when θ is obtained from σ by transposing a pair of consecutive values of σ ; a pair (σ_i, σ_j) such that $i < j$ and $\sigma_j = \sigma_i + 1$. For example, Figure 1.7 illustrates the weak order on \mathbb{S}_3 .

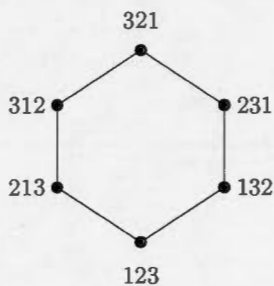


Figure 1.7: Weak order on \mathbb{S}_3 .

CHAPTER II

SOME CATALAN OBJECTS

Stanley (see [13]) has compiled a list of more than 207 combinatorial objects that are counted by the Catalan numbers. Much of our story concerns generalisations of the Catalan numbers and families of mathematical objects counted by these, which we call, *Catalan objects*. In this chapter we consider five families of Catalan objects: binary trees, complete binary trees, Dyck paths, Dyck words, and bounded increasing sequences. We count the number of Dyck paths to see it is equal to the Catalan numbers, and show that the other Catalan objects bijectively have the same cardinality.

2.1 Binary trees

Recall that a *tree* is an undirected, acyclic, connected graph. This means that any two nodes are connected by exactly one simple path. A *binary tree* is an arrangement of nodes and edges with *root* node on the top, and by descending, every node is connected to at most two nodes, which are said to be its right and left children. The root node separates the binary tree into two right and left subtrees. Let us denote by B_n the set of all binary trees with n nodes. The number of nodes of a binary tree is called the *size* of the tree. The cardinality of B_n is equal to $C(n)$. For example, Figure 2.1 shows the set of binary trees with three nodes.

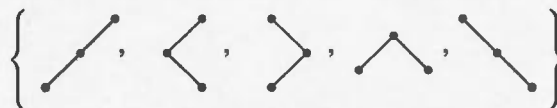


Figure 2.1: The set B_3 , of binary trees with 3 nodes.

2.2 Complete binary trees

A *complete binary tree* is a binary tree for which every node has either none or two children. Let us denote by C_n the set of all complete binary trees with $2n + 1$ nodes (or n internal nodes). The number of internal nodes of a complete binary tree is called the *size* of the tree. The cardinality of C_n is the same as the cardinality of B_n , thus they are in bijection. By adding new nodes to a binary tree so that each node is either a leaf (which has no children) or is an internal node (which has exactly two children), we can transform a binary tree into a complete binary tree. For example, Figure 2.2 shows the set of complete binary trees with seven nodes.

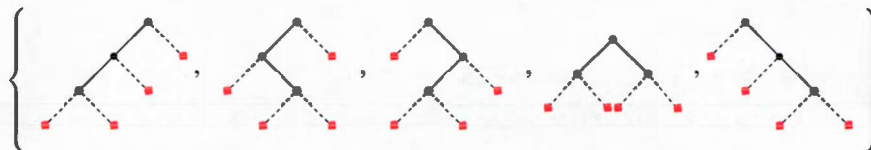


Figure 2.2: The set C_3 , of complete binary trees with 7 nodes.

2.3 Dyck paths

One of the other Catalan objects that we are interested in is the family of Dyck paths. A *Dyck path* of size n is a path in the $n \times n$ square consisting of only south and east steps of length one that the path doesn't pass above the line $y = -x + n$ in the grid. It starts at $(0, n)$ and ends at $(n, 0)$. A walk of length n along a Dyck path consists of $2n$ steps, with n in the south direction and n in the east direction. By necessity the first step must be a south step and the last one should be an east step. Let us denote by D_n the set of all Dyck paths of length n . For example, Figure 2.3 shows the set of Dyck paths of size three.

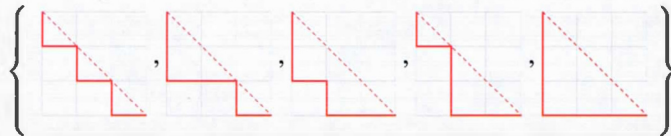


Figure 2.3: The set D_3 , of Dyck paths of size 3.

A consecutive sequence of r south steps is called a *vertical run* of length r . One single south step is a vertical run of length one, and the absence of south steps is a vertical run of length zero.

For a Dyck path $\alpha \in D_n$, $\gamma(\alpha) = a_1 a_2 \dots a_n$ is called the *composition* of α if the i -th vertical run of α has length a_i (for $1 \leq i \leq n$), and $\sum_{i=1}^n a_i = n$. Clearly $\gamma(\alpha)$ is a composition of n . For example, Figure 2.4 illustrates a Dyck path in D_3 with composition 21.



Figure 2.4: A Dyck path with composition 21 .

2.3.1 Count the number of Dyck paths

A random path in a square $n \times n$, is a path with $2n$ steps (n south steps and n east steps, each of length one) that starts at $(0, n)$ and ends at $(n, 0)$. Hence the total number of random paths with $2n$ steps is

$$\binom{2n}{n}.$$

A Dyck path is the special case of a random path which stays on or below the line $y = -x + n$. We will count the number of random paths that begin at $(0, n)$ and go above the line $y = -x + n$ at some point or totally (we call them, non-Dyck paths). Finally, by subtracting the number of non-Dyck paths from $\binom{2n}{n}$, we reach the number of Dyck paths. The non-Dyck paths hit the line $y = -x + (n + 1)$ at some point. If we take the first point where the path hits the line $y = -x + (n + 1)$, and reflect the rest of the path through that line, the reflected part ends at $(n + 1, 1)$ on the line $y = -x + (n + 2)$.

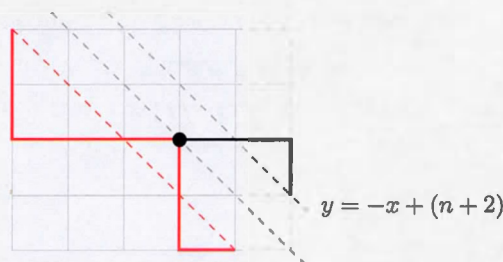


Figure 2.5: Non-Dyck path (in red), and its reflected part (in black) .

For example, Figure 2.5 illustrates a non-Dyck path that hits the line $y = -x + 5$ at $(3, 2)$, and shows its reflected path from this point with black.

Furthermore, any random path starting at $(0, n)$ and ending at $(n + 1, 1)$, after $2n$ steps must cross the line $y = -x + (n + 1)$ at some point, and by reflecting back up the black part, we reach the non-Dyck path. This bijection helps us to count the number of non-Dyck paths. In the second random path (which ends up at $(n + 1, 1)$), we need to take $(n - 1)$ south steps and $(n + 1)$ east steps out of $2n$, hence there are $\binom{2n}{n-1}$ of this type of paths. In conclusion we can count the number of Dyck paths as:

$$\begin{aligned} \#\text{Dyck paths} &= \binom{2n}{n} - \binom{2n}{n-1} \\ &= \frac{(2n)!}{n! n!} - \frac{(2n)!}{(n-1)! (n+1)!} \\ &= \frac{(2n)!}{(n-1)! n!} \left(\frac{1}{n} - \frac{1}{n+1} \right) \\ &= \frac{(2n)!}{(n-1)! n!} \left(\frac{1}{n(n+1)} \right) \\ &= \frac{1}{n+1} \frac{(2n)!}{n! n!} = C_n \end{aligned}$$

2.4 Dyck words

We can denote a Dyck path by a word $w_1 \dots w_{2n}$ which contain n copies of the letter S and contain n copies of the letter E , known as a *Dyck word* of length n . The letters S denotes the south steps $(0, 1)$ and letters E denotes the east steps $(1, 0)$. Clearly, this gives a bijection between Dyck paths and the mentioned words. For instance, the Dyck words correspond to Dyck paths of Figure 2.3 are respectively:

$$\{SESESE, SSEESE, SSESEE, SESSEE, SSSEE\}.$$

If a Dyck word is broken into two parts, the first part has at least as many S 's as E 's; this is equivalent to the condition "the path never passes above the line $y = -x + n$ " in Dyck paths.

Note that it is also common to show Dyck words by encoding them with 1 for south steps and 0 for east steps. For a given word $w = w_1 \dots w_{2n}$, if we denote the number of occurrences of the letter S by $|w|_S$ (resp. $|w|_E$ for letter E), then as a direct definition, we can see that a word w is a Dyck word if and only if

1. $w_i \in \{S, E\}$,
2. $|w_1 w_2 \dots w_i|_S \geq |w_1 w_2 \dots w_i|_E$, for all $1 \leq i \leq 2n$,
3. $|w|_S = |w|_E$.

2.5 Bijection between complete binary trees and Dyck paths

The set of Dyck paths of length n and the set of complete binary trees with n internal nodes have the same cardinality, $C(n) = \frac{1}{n+1} \binom{2n}{n}$, so there is a bijection between these two Catalan objects. In order to explain this bijection, we need the definition of a post-order. For a given complete binary tree, there are many ways for traversing its nodes, one of which is the *post-order*. The post-order starts traversing from the left most leaf, and the root node is visited after visiting the left and right subtrees. For example, the post-order traversal for the complete binary tree of Figure 2.6 is "e, f, g, d, h, c, b, i, a".

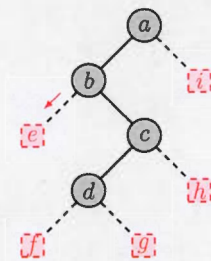


Figure 2.6: The post-order of this tree is e, f, g, d, h, c, b, i, a .

Since each child in a complete binary tree is hanging on an edge, so the post-order on nodes induces a post-order on those edges.

Now we introduce the bijection $f : C_n \rightarrow D_n$. For a given complete binary tree with n internal nodes, there are n edges going to the left and n edges going to the right. Now by using the post-order traversal on edges we can associate to a complete binary tree with n internal nodes the word that contains a letter S for the edges that are going to the left and a letter E for the edges that are going to the right. The resulting word is a Dyck word.

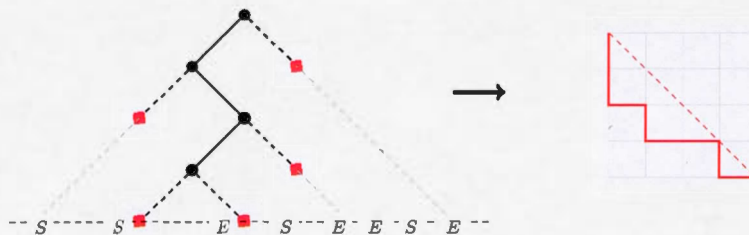


Figure 2.7: Transforming the complete binary tree to Dyck path.

We can obtain a Dyck path by translating S 's and E 's respectively into south and east steps. For example, Figure 2.7 shows the Dyck path of length four that is obtained from the complete binary tree with four internal nodes (we have shown its post-order traversal in Figure 2.6). Our inverse bijection $f^{-1} : D_n \rightarrow C_n$, is recursively constructed with two cases as follows. Consider two Dyck paths of Figure 2.8:

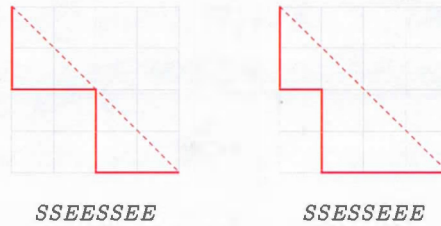


Figure 2.8: Dyck path which meets the diagonal (left one),
and does not meet the diagonal (right one).

The first Dyck path can be broken into two smaller Dyck paths, $SSEE|SSEE$, at the point that the path meets the diagonal $y = -x + 4$ (except the points $(4, 0)$ and $(0, 4)$). However, for the second Dyck path, there is no such a breaking point.

Case 1. The given Dyck path meets the diagonal $y = -x + n$ at points except $(n, 0)$ and $(0, n)$. So the Dyck path breaks into two smaller Dyck paths on the meeting point. In each smaller Dyck path by translating the S 's and E 's to left and right edges, we obtain the complete binary trees that correspond to them. Now in order to put them together, we attach the root of the first tree to the left most leaf of the second tree. If there is more than one break point, the algorithm continues recursively. For example, Figure 2.9 mentions that we can break $SESE$ into two Dyck path such as $SE|SE$. So by putting the root of the tree $f^{-1}(SE)$ on the left leaf of the tree $f^{-1}(SE)$, we get the tree $f^{-1}(SESE)$.

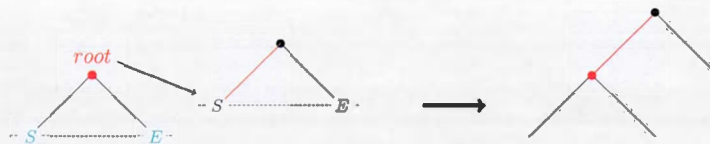


Figure 2.9: Transforming the Dyck path $SESE$ to a complete binary tree.

Case 2. The given Dyck path does not meet the diagonal $y = -x + n$ except at the points $(n, 0)$ and $(0, n)$. Since the first step in the Dyck path is always a south step and the last one is an east step, its corresponding Dyck word is SME where the middle part M is a smaller Dyck path. Now the algorithm is: construct the complete binary tree for the middle word M , then attach it to the right edge of the tree $f^{-1}(SE)$, as it is shown in Figure 2.10.

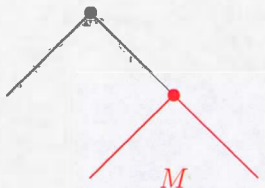


Figure 2.10: General form of transforming Dyck path SME to a complete binary tree.

Note that constructing the tree $f^{-1}(M)$ might involve applying the algorithm of case 1 (if $M = \square|\square$) or again by applying the algorithm of case 2 (if $M = SM'E$). For example, the Dyck path $SSESESEEE$ does not cross the diagonal, so first we make the tree for $M = SESESE$ and then add it to the right edge of the tree $f^{-1}(ES)$. Here building the tree for M is by applying the algorithm of case 1 ($M = SE|SE|SE$). The result is shown in Figure 2.11.



Figure 2.11: Transforming the Dyck path $SSESESEEE$ to a complete binary tree.

2.6 Bounded increasing sequences

We say that $\beta = (b_1, \dots, b_n)$ is a *bounded increasing sequence* if $b_i \leq b_j$ and $b_i \leq i$ for all $1 \leq i, j \leq n$. They may be used to bijectively encode Dyck paths. This means that the set of Dyck paths of size n are in bijection with the set of mentioned sequence $(b_1 \leq b_2 \leq \dots \leq b_n)$. For a given sequence, let r_i

be the number of times that i occurs in the sequence. Then we associate the following Dyck path to the sequence:

$$\overbrace{S \dots S}^{r_1} E \overbrace{S \dots S}^{r_2} E \dots \overbrace{S \dots S}^{r_n} E.$$

Here, S denotes a south step $(0, 1)$, and E denotes an east step $(1, 0)$. For example, as Figure 2.12 shows, the weakly increasing sequence $1 \leq i_1 \leq i_2 \leq i_3$ corresponds to the Dyck path $SSSEEESE$:

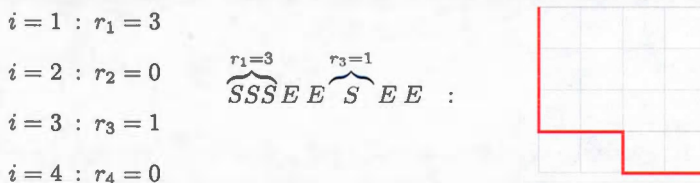


Figure 2.12: Sequence $(1, 1, 1, 3) \rightarrow$ Dyck path $SSSEEESE$.

Our inverse bijection, is constructed as follows. For a given Dyck path, the length of i -th vertical run is the number of occurrences of i in the corresponding bounded increasing sequence. For example, for the Dyck path of Figure 2.13, $\ell(r_1) = 2, \ell(r_2) = 0, \ell(r_3) = 1, \ell(r_4) = 1$. This means that in the bounded increasing sequence 1 occurs two times, 2 does not occur, 3 occurs once, and 4 occurs once so corresponding sequence is 1134.

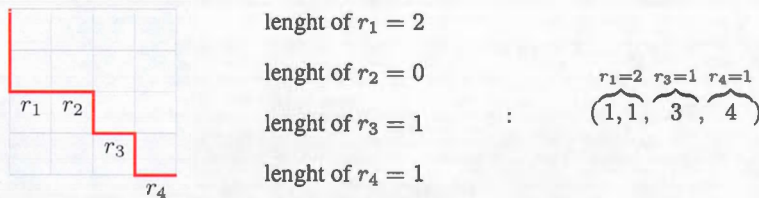


Figure 2.13: Dyck path $SSEEESE$ \rightarrow sequence $(1, 1, 3, 4)$.

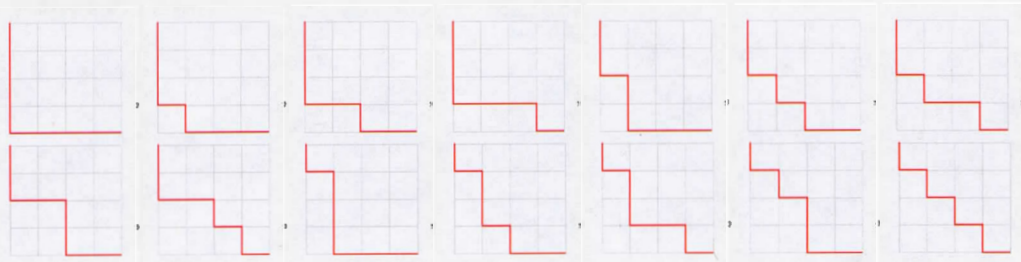
Let us denote by \mathcal{B}_n the set of such sequences, which is enumerated by the Catalan numbers. For instance in the following we show some bounded increasing sequences of length 1, 2, 3 and 4 that encode Dyck paths of the same length.

$$\mathcal{B}_1 = \{(1)\} : \quad \text{[Diagram: A single square grid with a red path starting at the top-left corner and ending at the bottom-right corner, consisting of one horizontal segment and one vertical segment.]}$$

$$\mathcal{B}_2 = \{(1,1), (1,2)\} : \quad \text{[Diagram: Two square grids. The first has a red path starting at the top-left, going right, then down, then right. The second has a red path starting at the top-left, going down, then right, then down.]}$$

$$\mathcal{B}_3 = \{(1,1,1), (1,1,2), (1,1,3), (1,2,2), (1,2,3)\} : \quad \text{[Diagram: Five square grids showing various red paths with three steps.]}$$

$$\mathcal{B}_4 = \{(1,1,1,1), (1,1,1,2), (1,1,1,3), (1,1,1,4), (1,1,2,2), (1,1,2,3), (1,1,2,4), (1,1,3,3), (1,1,3,4), (1,2,2,2), (1,2,2,3), (1,2,2,4), (1,2,3,3), (1,2,3,4)\} : \quad \text{[Diagram: Fourteen square grids showing various red paths with four steps.]}$$



There are more than 200 other such bijections between the families of mathematical objects counted by Catalan numbers. Later in Chapter 5, we will see that the set of "maximal tubings of path graphs" is in bijection with the set of complete binary trees.

CHAPTER III

TAMARI POSET ON CATALAN OBJECTS

In this chapter we introduce the notion of Tamari lattice, and two of its realizations. First as a poset on complete binary trees, and then on Dyck paths. Furthermore, we explicitly describe the covering relation for the families of Catalan objects previously considered in Chapter 2. We also count the number of intervals of Tamari posets, by using the zeta polynomial to count the number of chains in the Tamari poset.

3.1 Tamari poset

One of the interesting lattices in combinatorics is the Tamari lattice, introduced by Dov Tamari. Tamari in his thesis [14, 1951], considered the set of well-formed parentheses strings of length $2n$ with n open, and n closed parentheses such that each opening parenthesis has a uniquely associated closing parenthesis at its right. For instance, the possible well-formed parentheses strings of length 6 with those condition are $()()()$, $((()))$, $()(())$, $((())$, $((())$. Later in [15, 1962], he partially ordered this set with the covering relation $()() \rightarrow ((())$, in the right-to-left direction. This poset with the described relation is a lattice that is know as the *Tamari lattice*, denoted \mathcal{T}_n . The property that makes the Tamari lattice one of the most controversial issues of combinatorics is its cardinality that is given by the n -th Catalan number:

$$\text{Number of elements of } \mathcal{T}_n = \frac{1}{n+1} \binom{2n}{n}.$$

These lattices possess realizations as special polytopes¹, called "associahedra", which appeared in Stash-eff's thesis in 1961. Thus the 1-skeleton² of the n -dimensional "associahedron" corresponds to the Hasse diagram of \mathcal{T}_n (see [10] for more details). For example, Figure 3.1 indicates the Tamari lattice \mathcal{T}_3 which has five elements.

¹A *polytope* is a geometric object with flat sides that exists in any number of dimensions.

²*1-skeleton* of a polytope is the set of vertices and edges of that polytope.

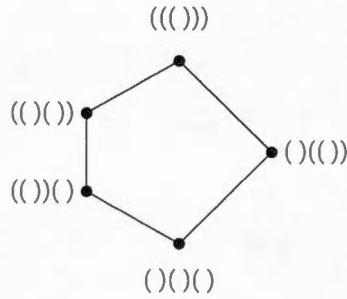


Figure 3.1: The Tamari lattice \mathcal{T}_3 .

There are many realizations of the Tamari lattice as a partial order on "Catalan objects". In this chapter, we will study the covering relations in posets of complete binary trees, Dyck paths, and Dyck words. It is clear that, by the bijection between complete binary trees and Dyck paths, the Tamari lattice of one can be obtained from the other.

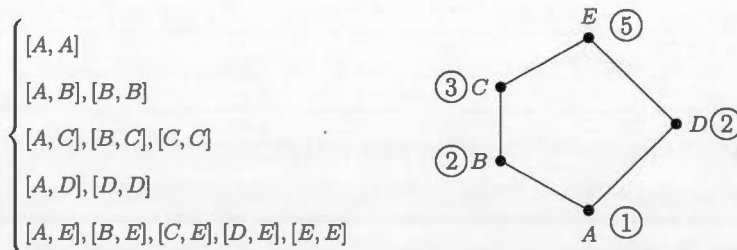
The first result about the intervals of the Tamari lattice (i.e. pairs $[P, Q]$ such that $P \preceq Q$ for $P, Q \in \mathcal{T}_n$) was from Chapoton in [6]. He proved that intervals in the Tamari lattice are enumerating by the following formula:

$$\text{Number of Intervals of } \mathcal{T}_n = \frac{2}{n(n+1)} \binom{4n+1}{n-1}, \tag{3.1.1}$$

which gives the following sequence:

1, 3, 13, 68, 399, 2530, ... (see <https://oeis.org/A000260>)

For example, for the Tamari poset \mathcal{T}_3 in Figure 3.2, the number near each vertex is the number of intervals with that vertex the top of the interval. Hence the total number of intervals in \mathcal{T}_3 is $1+2+3+5+2 = 13$ that satisfies equation (3.1.1) for $n = 3$.



- $$\left\{ \begin{array}{l} [A, A] \\ [A, B], [B, B] \\ [A, C], [B, C], [C, C] \\ [A, D], [D, D] \\ [A, E], [B, E], [C, E], [D, E], [E, E] \end{array} \right.$$

Figure 3.2: The enumeration of intervals in Tamari lattice \mathcal{T}_3 .

Also, we can calculate the zeta polynomial by equation (1.2.1) for Tamari posets. For instance we have

$$Z_{\mathcal{T}_1}(n) = 1.$$

$$Z_{\mathcal{T}_2}(n) = 1 + n.$$

$$Z_{\mathcal{T}_3}(n) = n + 3\binom{n}{2} + \binom{n}{3}.$$

$$Z_{\mathcal{T}_4}(n) = n + 12\binom{n}{2} + 29\binom{n}{3} + 26\binom{n}{4} + 11\binom{n}{5} + 2\binom{n}{6}.$$

⋮

Table 3.1 illustrates some values of the zeta polynomial for Tamari posets, denoted $Z_{\mathcal{T}_i}(k)$. The second column of the table is the Catalan sequence which counts the number of multi-chains from $\hat{0}$ to $\hat{1}$ of length two in each Tamari poset. The third column of table is the sequence 3.1.1 that counts the number of intervals of each Tamari.

$i \backslash k$	1	2	3	4	5
1	1	1	1	1	1
2	1	2	3	4	5
3	1	5	13	26	45
4	1	14	68	218	556

Table 3.1: Some values of the zeta polynomials for the Tamari posets $\mathcal{T}_1, \mathcal{T}_2, \mathcal{T}_3$, and \mathcal{T}_4 .

3.2 Tamari poset on binary trees

The Tamari order on the poset of binary trees is *rotation* operation. As it is shown in Figure 3.3, if a complete binary tree T is composed of a root " \bullet ", and a left subtree " \bullet ", then the right rotation of t on " \bullet " means replacing $(A \bullet B) \bullet C$ by $A \bullet (B \bullet C)$ in T (note that A, B or C might be empty). Hence, this is associativity.



Figure 3.3: Right-rotation.

Consider two complete binary trees t_1 and t_2 of the same size. We say that t_2 covers t_1 in the Tamari lattice if and only if t_2 can be obtained by a sequence of right rotations from t_1 . Figure 3.4 shows this notion.

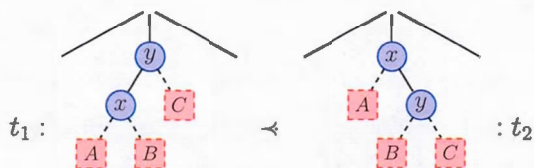


Figure 3.4: Notion of $t_1 \prec t_2$.

The set of complete binary trees of size n with the Tamari order is in fact a lattice. For example, Figure 3.5 shows the Tamari lattice for $n = 3$ and $n = 4$.

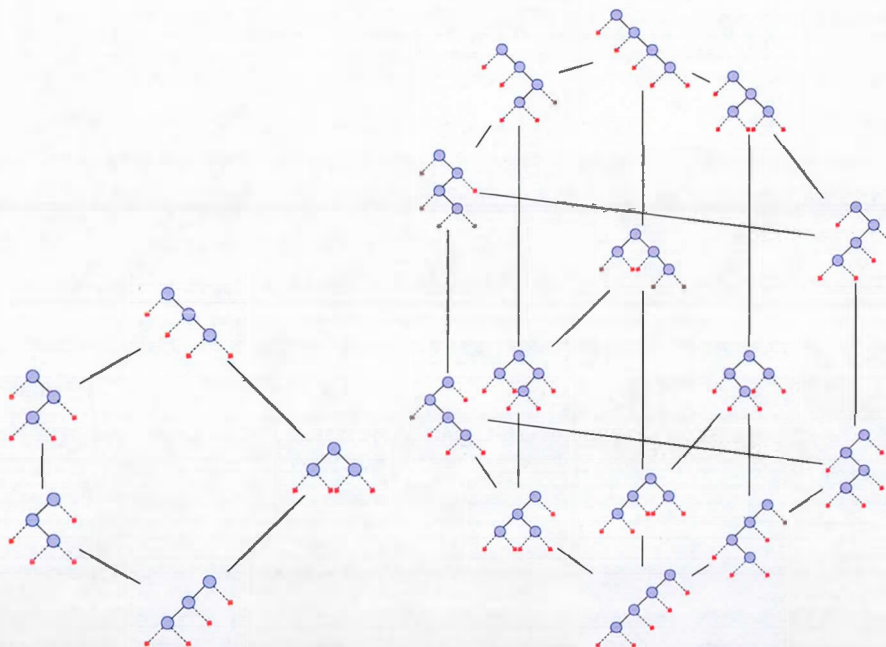


Figure 3.5: The Tamari lattice of complete binary trees for $n = 3$ (left) and $n = 4$ (right).

Since complete binary trees correspond bijectively to binary trees, we clearly have an equivalent description of Tamari lattice in terms of the latter. Thus we get the representations in Figure 3.6.

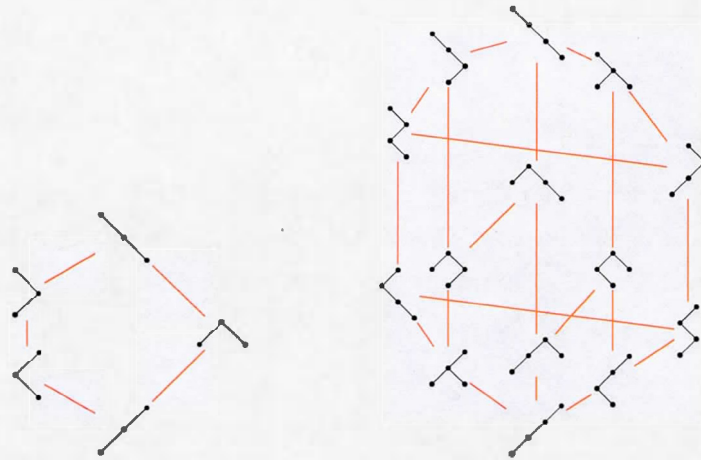


Figure 3.6: The Tamari lattice of binary trees for $n = 3$ (left) and $n = 4$ (right).

3.3 Tamari poset on Dyck paths

Consider two Dyck paths d_1 and d_2 of the same size. We say that d_2 covers d_1 if and only if there exists in d_1 an east step a , and a south step b following a , such that d_2 is obtained from d_1 by swapping a and F , where F is the shortest factor of d_1 that begins with b and is a Dyck path. Figure 3.7 shows this notion.



Figure 3.7: Notion of $d_1 \prec d_2$.

The set of Dyck paths of size n with the Tamari order is in fact a lattice. For example, Figure 3.8

represents the Tamari lattice for $n = 3$ and $n = 4$.

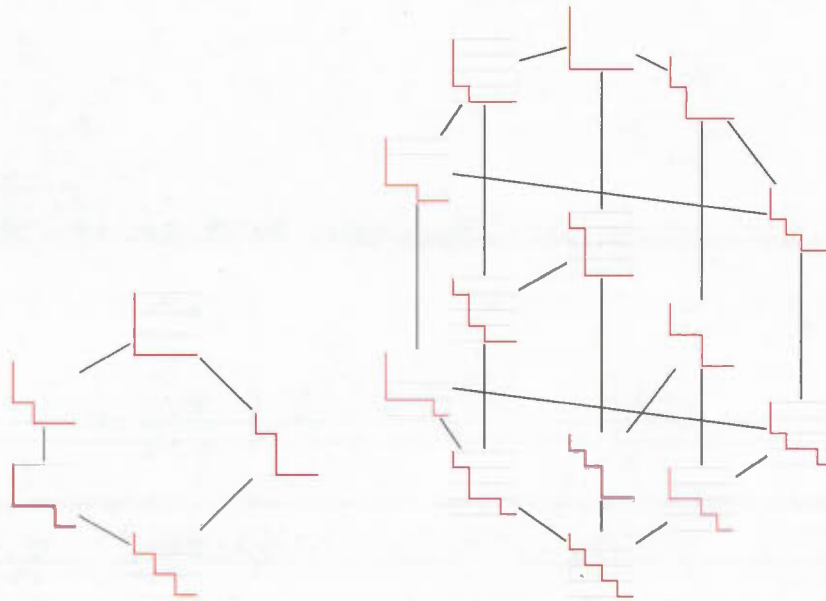


Figure 3.8: The Tamari lattice of Dyck paths for $n = 3$ (left) and $n = 4$ (right).

3.4 Tamari poset on Dyck words

Consider two Dyck words w_1 and w_2 of the same length. We say that w_2 covers w_1 if and only if there exists in w_1 a letter S following E , such that w_2 is obtained by changing the place of E and F , where F is the shortest factor of w_1 that begins with S , and is a Dyck word. For example the two Dyck words $w_1 = SSSEESSEEESE$ and $w_2 = SSSESSEEESE$, which correspond to the Dyck paths of Figure 3.5, illustrates the notion of $w_1 \prec w_2$:

$$SSSE \underbrace{ESSEE}_{F} SE \prec SSSE \underbrace{SSEE}_{F} ESE.$$

The set of Dyck words of size n with the Tamari order is in fact a lattice.

Clearly, one can transfer the poset structure from that on Dyck paths to any other Catalan family using an explicit bijection. Hence, for D_n as a set of Dyck paths and C_n as a set of other Catalan objects, one sets

$$\theta(\alpha) \preceq \theta(\beta) \text{ if and only if } \alpha \preceq \beta$$

for $\alpha, \beta \in D_n$, and $\theta : D_n \rightarrow C_n$ a bijection.

However, a direct description of the order on C_n is often preferred.

For example, let T be a triangulation of a polygon (which is counted by Catalan numbers) such as Figure 3.9. Within T , the diagonal t is the diagonal of some quadrilateral. Then there is a new triangulation T' which is obtained by replacing the diagonal t with the other diagonal of that quadrilateral. This local move is called an *edge flip*, and we say that T' is obtained from T by flipping the diagonal t .

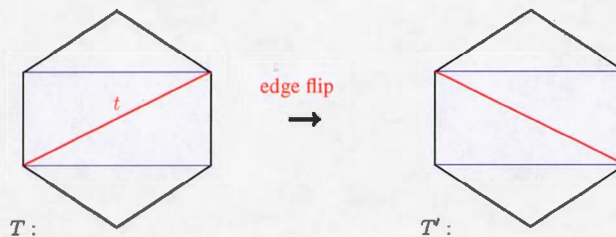


Figure 3.9: Two triangulations T and T' are being related by an edge flip.

This case is interesting since it plays a crucial role in the origin of the notion of "cluster algebras" (see [16] for more details).

Then the question emerges that,

Is there some systematic way to think about "flips" in the Tamari poset of Catalan objects?

In Chapter 5, we are going to introduce what is the Tamari order for the notion of "tubing", as a main goal of the current study.

CHAPTER IV

PARKING FUNCTIONS ON CATALAN OBJECTS

In this chapter we introduce the notion of parking functions, and some of their properties. Here our interest is in associating parking functions to Catalan objects. Hence we can identify a parking function with a labeled Dyck path, Dyck word, and complete binary tree. The bijection between parking functions and labeled Dyck paths lead to the creation of labeled intervals in the Tamari lattice of Dyck paths. On the other hand, we try to enumerate parking functions with zeta polynomial.

4.1 Parking functions

The notion of "parking function" was introduced by Konheim and Weiss. In [9], they proved that the number of parking functions of length n is

$$(n + 1)^{n-1}.$$

Later, other combinatorialists gave some methods of counting the number of parking functions of length n , or introduced bijections relating parking functions to other combinatorial structures. The parking problem was described in [2] as the following story:

"Imagine a one-way street with n parking spots and a cliff at its end. We'll give the first parking spot number 1, the next one number 2, etc..., and the last one number n . At first all of them are free and there are n cars on the street, and they would all like to park. Every car has a parking preference, and we record the preferences in a sequence, for example, if $n = 3$, the sequence $(2, 1, 1)$ means that the first car would like to park at spot number 2, the second car prefers parking spot number 1, and the last car would also like to park at number 1. The street is narrow, so there is no way to back up. Now each three car in the street start to park on its preferred parking spot; if it is free, it parks there, and if not, it can go to the first available spot. We call a sequence a *parking function* (of length n) if all cars find a parking spot at the end and none fall off the cliff". For example, the sequence $(2, 1, 1)$ is a parking function (of

length 3), while the sequence $(1, 3, 3)$ is not, because car number 1 parks at spot number 1 as he prefers, car number 2 parks at spot number 3 and finally when car number 3 arrives to spot number 3 which is his preference, he finds it full and falls. In the other form of writing we say that 211 is a parking function (of length 3), while 133 is not. So a *parking function* is a sequence (a_1, a_2, \dots, a_n) of positive integers whose non-decreasing rearrangement (b_1, b_2, \dots, b_n) satisfies $b_i \leq i$.

Another interesting characterization of parking functions is the following:

A parking function of length n is a function $f : \{1, 2, \dots, n\} \rightarrow \{1, 2, \dots, n\}$ such that

$$|\{x : f(x) \leq i\}| \geq i \quad \text{for } 1 \leq i \leq n.$$

We think of the elements x in the domain of f as cars that wish to park, and the number $f(x)$ represents the spot where car x prefers to park. For example, Figure 4.1 illustrates that 211 is a parking function:

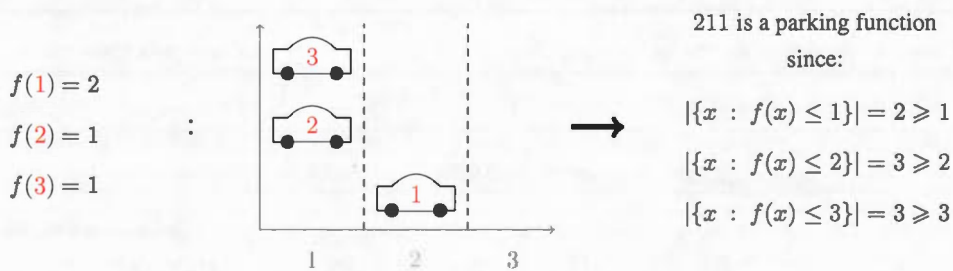


Figure 4.1: 211 is a parking function of length 3.

As the same story, function f is a parking function if and only if all n cars are able to park. This notation of parking functions of length n is more useful in the next section, when we consider a set of cars prefer spot i to park as elements of i -th vertical run of the Dyck paths of size n in connection of parking functions and Dyck paths.

We denote by P_n the set of all parking functions of length n . For example the number of parking functions of length 3 is $(3 + 1)^{3-1} = 16$ such as the following:

(1, 1, 1)
 (1, 1, 2) (1, 2, 1) (2, 1, 1)
 (1, 1, 3) (1, 3, 1) (3, 1, 1)
 (1, 2, 2) (2, 1, 2) (2, 2, 1)
 (1, 2, 3) (1, 3, 2) (2, 1, 3) (2, 3, 1) (3, 1, 2) (3, 2, 1)

This suggests to us that every permutation of the entries of a parking function is also a parking function,

meaning that for a symmetric group \mathbb{S}_n of degree n we have the following action on the set of parking functions of length n

$$\mathbb{S}_n \times P_n \rightarrow P_n$$

$$\sigma, \pi \mapsto \sigma \cdot \pi := (a_{\sigma(1)}, a_{\sigma(2)}, \dots, a_{\sigma(n)}). \quad (4.1.1)$$

where $\pi = (a_1, a_2, \dots, a_n)$ is an element of P_n , and $\sigma \in \mathbb{S}_n$. On the other hand, each orbit of this action contains exactly one bounded increasing sequence (see Section 2.6 for definition). Hence we identify each orbit by its associated bounded increasing sequence β , denoted P_β , such that

$$P_\beta := \{\pi \mid \pi = (a_{\sigma(1)}, a_{\sigma(2)}, \dots, a_{\sigma(n)}) \text{ for some } \sigma \in \mathbb{S}_n\}.$$

For example, for parking functions of length 3 we have:

$$P_{(1,1,1)} = \{(1, 1, 1)\}$$

$$P_{(1,1,2)} = \{(1, 1, 2), (1, 2, 1), (2, 1, 1)\}$$

$$P_{(1,1,3)} = \{(1, 1, 3), (1, 3, 1), (3, 1, 1)\}$$

$$P_{(1,2,2)} = \{(1, 2, 2), (2, 1, 2), (2, 2, 1)\}$$

$$P_{(1,2,3)} = \{(1, 2, 3), (1, 3, 2), (2, 1, 3), (2, 3, 1), (3, 1, 2), (3, 2, 1)\}$$

For β of length n , the number of elements that each P_β contains is

$$|P_\beta| = \frac{n!}{|\text{stab}_\beta|},$$

where $\text{stab}_\beta := \{\sigma \in \mathbb{S}_n \mid \sigma \cdot \beta = \beta\}$, and as in (4.1.1), for a bounded increasing sequence $\beta = (b_1, \dots, b_n)$ we have $\sigma \cdot \beta = (b_{\sigma(1)}, \dots, b_{\sigma(n)})$. For any $\beta = (\underbrace{1, 1, \dots, 1}_{n_1}, \underbrace{2, 2, \dots, 2}_{n_2}, \dots, \underbrace{k, k, \dots, k}_{n_k})$ that contains n_1 copies of element 1, n_2 copies of element 2, ..., and n_k copies of element k , the stabilizer of β is isomorphic to the Young subgroup of \mathbb{S}_n , therefore $|\text{stab}_\beta| = n_1!n_2!\dots n_k!$. Then we have

$$|P_\beta| = \frac{n!}{n_1!n_2!\dots n_k!} = \binom{n}{n_1, n_2, \dots, n_k}.$$

For example, for $\beta = (\underbrace{1, 1}_{n_1}, \underbrace{2}_{n_2})$:

$$|P_\beta| = \frac{3!}{2!1!} = 3.$$

We are going to make the action of the symmetric group on the set of parking functions more explicit in the next sections.

For example, for the Dyck path of Figure 4.3, there are exactly three labeled Dyck paths, so we have three parking functions associated with this Dyck path.

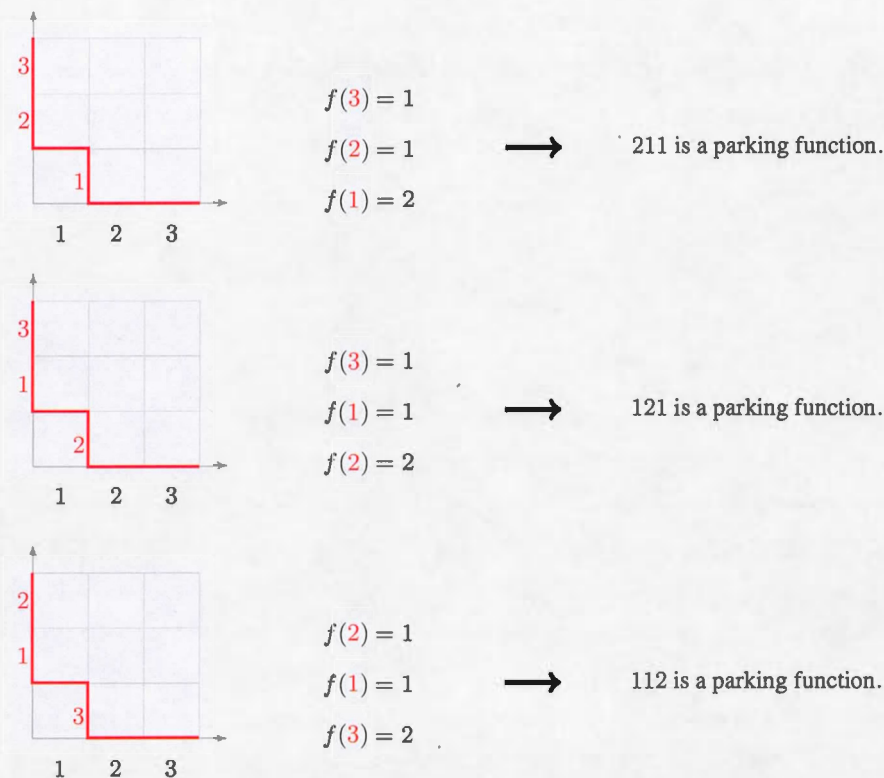


Figure 4.3: Parking functions over one Dyck path of size 3 .

Furthermore, we can identify a parking function f with a labeled Dyck path. For a given parking function, let $V_i = \{x : f(x) = i\}$ be the set of cars preferring spot i . Consider an n by n lattice square and start from top row to put the elements of V_1 in decreasing order in the first column of the lattice square, one per row. Similarly, put the elements of V_2 in the second column, and continue until V_n . Finally draw the vertical steps left of labels, and add the necessary horizontal steps to get a lattice path from $(0, n)$ to $(n, 0)$. The resulting labeled lattice path is a labeled Dyck path if and only if f is a parking function.

On the other hand, we want to count the number of labeled Dyck paths directly, and show that the cardinality of this set is equal to $(n+1)^{\binom{n-1}{n}}$.

For a Dyck path $\alpha \in D_n$, the number of such labelings is $\binom{n}{\gamma(\alpha)}$, where $\gamma(\alpha)$ is the composition of α . For example, for the Dyck path of Figure 4.3, as we observed, there are exactly $\binom{3}{2,1} = 3$ such labelings.

As Garsia and Haiman discussed implicitly in symmetric functions, and Armstrong, Loehr and Warrington retell in [1], the number of Dyck paths with r_i vertical runs of length i is equal to

$$\frac{1}{n+1} \binom{n+1}{r_0, r_1, r_2, \dots, r_n},$$

where we define r_0 so that $\sum_{i=0}^n r_i = n+1$, more specifically, $r_0 = n+1 - \ell(\gamma(\alpha))$. For example when $n=3$, there are three Dyck paths with specification $(r_1=1, r_2=1, r_3=0)$, so $r_0=2$, as shown in Figure 4.4.



Figure 4.4: Enumeration of Dyck paths with $(r_1=1, r_2=1, r_3=0)$.

Hence the number of labeled Dyck paths of size n or in other words the number of parking functions over Dyck paths of size n is equal to

$$\sum_{\substack{\gamma(\alpha) \\ \alpha \in D_n}} \frac{1}{n+1} \binom{n+1}{r_0, r_1, r_2, \dots, r_n} \binom{n}{\gamma(\alpha)}.$$

For example there are 16 parking functions over Dyck paths of D_3 :

$$\begin{aligned} & \overbrace{\frac{1}{4} \binom{4}{1, 3, 0, 0} \binom{3}{1, 1, 1}}^{\gamma(\alpha)=111} + \overbrace{\frac{1}{4} \binom{4}{2, 1, 1, 0} \binom{3}{2, 1}}^{\gamma(\alpha)=21} + \overbrace{\frac{1}{4} \binom{4}{3, 0, 0, 1} \binom{3}{3}}^{\gamma(\alpha)=3} \\ & = 1 \times 6 + 3 \times 3 + 1 \times 1 = 16, \end{aligned}$$

which is the same as the number of parking functions of length three: $(n+1)^{n-1} = (3+1)^{3-1} = 16$.

4.2.1 Labeled intervals

Let \mathcal{T}_n be the Tamari lattice of Dyck paths of size n . In Chapter 3 we introduced the number of intervals of the Tamari lattice. Now we are going to study the number of labeled intervals of the Tamari lattice.

From Section 4.2 we know that the number of labeled Dyck paths is $(n+1)^{n-1}$. The symmetric group \mathbb{S}_n acts on labeled Dyck paths by permuting labels, and then reordering them in such a way that labels are

decreasing along the vertical runs. For example, Figure 4.5 illustrates how $\sigma = 3214$ as a permutation in \mathbb{S}_4 acts on $d \in D_4$:

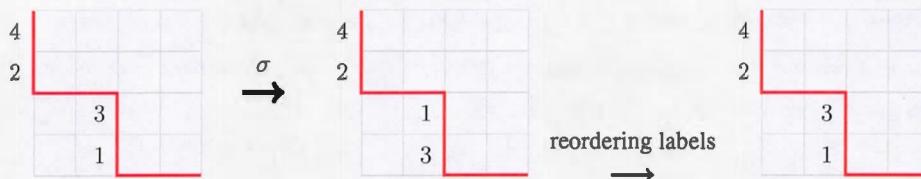


Figure 4.5: How σ permutes the labels of a labeled Dyck path of D_4 .

Note that in this example, labels are not changed after permutation and reordering. Suppose that $\sigma \in \mathbb{S}_n$ has a cycle decomposition $\sigma = \sigma_1 \sigma_2 \dots \sigma_k$, which is the product of k disjoint cycles of length $\lambda_1, \lambda_2, \dots, \lambda_k$ respectively. The number of labeled Dyck paths whose labels are stable by σ is

$$(n + 1)^{k-1}.$$

For example, consider the Tamari lattice of D_3 with all 16 possible labeled Dyck paths. For $\sigma = 132 = (1)(32)$, there are four labeled Dyck paths that have stable labels under σ , which are shown in Figure 4.6. The formula gives the same result by putting $k = 2$ because σ decomposes into two disjoint cycles.



Figure 4.6: Stable labeled Dyck paths of D_3 by σ .

For two Dyck paths $d, d' \in D_n$, An interval $[d, d']$ of \mathcal{T}_n is called *labeled interval* if the upper path d' is labeled Dyck path. The number of labeled Tamari intervals whose labels are stable by σ is

$$(n + 1)^{k-2} \prod_{i \geq 1} \binom{2i}{i}^{\beta_i},$$

if σ has β_i cycles of length i for $i \geq 1$ and k cycles in total.

For example, in the Tamari lattice of D_3 , for $\sigma = 132 = (1)(32)$ that has one cycle of length one, and

one cycle of length two, the formula gives 12 labeled intervals. On the other hand, as we mentioned in Figure 4.6, there are four labeled Dyck paths that are stable under $\sigma = 132$, and in the Tamari poset of D_3 the number of intervals when each of these four paths is the top point of the interval, are 5, 2, 3, and 2 respectively. Therefore, we have $5 + 2 + 3 + 2 = 12$ labeled intervals stable by σ .

In particular, when σ is the identity permutation, then $\sigma = (1)(2)\dots(n)$, the product of n disjoint cycles of length one, hence total number of labeled intervals is

$$2^n(n + 1)^{n-2}.$$

In this case, σ keeps the order of labels of labeled Dyck paths, therefore in the labeled interval $[d, d']$, all the possible labeled forms for d' is counted (see [4] for more informations).

For example, for the Tamari lattice of Dyck paths size three, the number of labeled intervals is 32. Beside the mentioned formula, there is an interesting explanation for that. Figure 4.7, illustrates a Tamari poset \mathcal{T}_3 of Dyck paths of size three, that in part (a) the number near each vertex is the number of possible labeled Dyck paths for that element, and in part (b) the number near each vertex is the number of intervals when that element is the top (see Figure 3.2, Chapter 3). Finally in part (c), the number near each vertex is the number of labeled intervals (stable by identity permutation) when that element is the top.

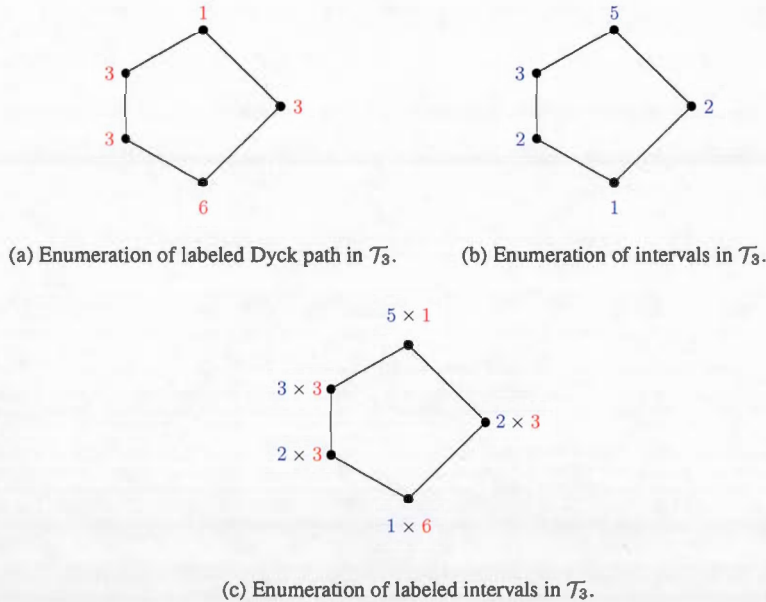


Figure 4.7

4.3 Parking functions on Dyck words

To associate a parking function with a Dyck word of size n , we put labels $\{1, 2, \dots, n\}$ on the letters S , so that each consecutive sequence of letters S have labels in decreasing order. For example, consider the Dyck word $SSESEE$, which corresponds to the Dyck path of Figure 4.1. There are exactly three labelings for this Dyck word which satisfy the above condition:

$$\overset{3}{S} \overset{2}{S} \overset{1}{E} S E E, \quad \overset{3}{S} \overset{1}{S} \overset{2}{E} S E E, \quad \overset{2}{S} \overset{1}{S} \overset{3}{E} S E E$$

For each such labeling, we can obtain a parking function f by setting $f(x) = i$ if and only if label x occurs in i -th consecutive sequence of letters S such as the following:

$$\underbrace{S \dots S}_{f(\text{labels})=1} E \underbrace{S \dots S}_{f(\text{labels})=2} E \dots \underbrace{S \dots S}_{f(\text{labels})=n} E.$$

For example, the parking functions over the Dyck word $SSESEE$ are:

$$\begin{aligned} \overset{3}{S} \overset{2}{S} \overset{1}{E} S E E &\rightarrow \begin{cases} f(3) = 1 \\ f(2) = 1 \\ f(1) = 2 \end{cases} \rightarrow 211 \text{ is a parking function.} \\ \overset{3}{S} \overset{1}{S} \overset{2}{E} S E E &\rightarrow \begin{cases} f(3) = 1 \\ f(1) = 1 \\ f(2) = 2 \end{cases} \rightarrow 121 \text{ is a parking function.} \\ \overset{2}{S} \overset{1}{S} \overset{3}{E} S E E &\rightarrow \begin{cases} f(2) = 1 \\ f(1) = 1 \\ f(3) = 2 \end{cases} \rightarrow 112 \text{ is a parking function.} \end{aligned}$$

Further, for a given parking function, let $V_i = \{x : f(x) = i\}$ be the set of cars preferring spot i . We start with V_1 and rewrite its elements in decreasing order and correspond a letter S to each of them, then immediately put a letter E to finish our first sequence of letters S . We continue until V_n , and the resulting sequence of letters S and E is a labeled Dyck word.

4.4 Parking functions on complete binary trees

To associate a parking function with a complete binary tree with n internal nodes, we use post-order traversal to put labels $\{1, 2, \dots, n\}$ on edges. According to the definition of post-order, we start traversing the tree from the first most left edge and for a consecutive sequence of left edges in traverse, their labels should be in decreasing way. The single left edges are free in labeling. For example, Figure 4.8, shows three different labelings of the complete binary tree which is equal to the Dyck path of Figure 4.3.

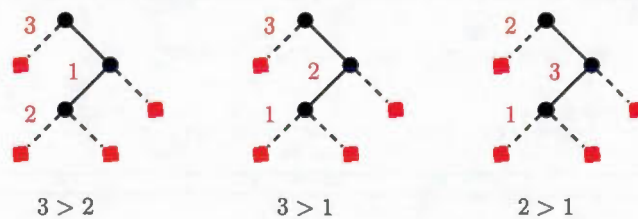
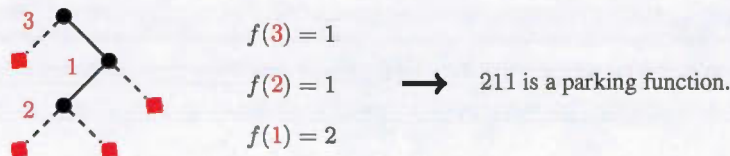


Figure 4.8: Parking functions over a complete binary tree of C_3 .

If, as before, we associate the letter S to the edges that goes to the left, and the letter E to the edges going to the right, then for each labeling of the complete binary tree we get a parking function f by setting $f(x) = i$ if and only if label x occurs in i -th sequence of left edges in the post-order traversal such as the following:

$$\underbrace{S \dots S}_{f(\text{labels})=1} \ E \ \underbrace{S \dots S}_{f(\text{labels})=2} \ E \dots \ \underbrace{S \dots S}_{f(\text{labels})=n} \ E.$$

This means that the value of f is identical for the elements of each sequence, and from the first sequence of left edges to the second sequence by passing just one right edge, the value of f augments just one unit while by passing i right edges, augments i units. For example, Figure 4.9, illustrates the parking functions on the complete binary trees that we have labeled in Figure 4.8.



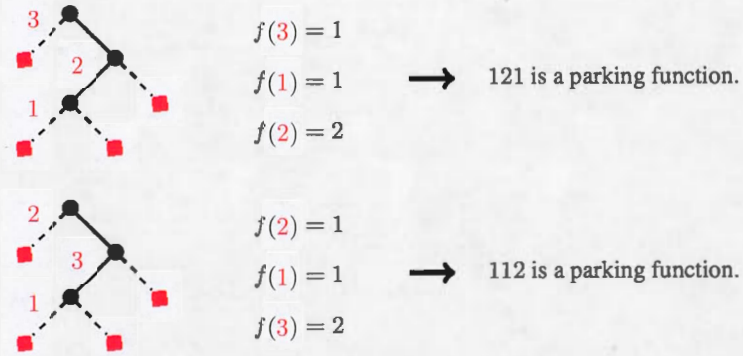


Figure 4.9: Parking functions over one complete binary tree of size 3 .

However, for a given parking function, obtaining the labeled complete binary tree directly is difficult but bijections of Chapter 2 can help us. For example, one can first obtain a related Dyck word then translate that into a complete binary tree.

4.5 Zeta polynomial for parking functions enumeration

According to Section 4.2, we can associate parking functions with the elements of the Tamari poset of Dyck paths (it comes from Section 2.6, we associated bounded increasing sequences with Dyck paths). Hence we can study how the zeta polynomial can enumerate the mentioned parking functions.

For a Tamari poset P_{\leq}^n of Dyck paths of size n , we define $\mathcal{C} = (\beta_1, \beta_2, \dots, \beta_k)$, a sequence of length k of bounded increasing sequences $\beta_i = (a_1, a_2, \dots, a_n)$, such that $\hat{0} = \beta_1 \preceq \beta_2 \preceq \dots \preceq \beta_k$. Let P_{β_i} be the set of parking functions associated to β_i . The same as counting the multi-chains in zeta polynomials (see equation (1.2.1)), here we count the pairs (\mathcal{C}, π) in $Y_n(k)$ defined as follows:

$$Y_n(k) := \#\{(\mathcal{C}, \pi) \mid \mathcal{C} = (\beta_1, \beta_2, \dots, \beta_k) \text{ with } \beta_1 = \hat{0} \text{ and } \pi \in P_{\beta_k}\}.$$

We can see that $Y_n(k)$ is a polynomial in k , since for each $\mathcal{C} = (\beta_1, \beta_2, \dots, \beta_k)$ there exists a sequence $\mathcal{D} = (\beta_1, \beta_2, \dots, \beta_j)$ length $j - 1$ such that $\hat{0} = \beta_1 \prec \beta_2 \prec \dots \prec \beta_j = \beta$, hence

$$\begin{aligned} Y_n(k) &= \sum_{j=1}^k \binom{k-1}{j-1} \sum_{\mathcal{D}} \#P_{\beta} \\ &= \sum_{j=1}^k \binom{k-1}{j-1} \sum_{\mathcal{D}} \frac{n!}{|\text{stab}_{\beta}|}. \end{aligned} \quad (4.5.1)$$

For example, Figure 4.10 illustrates the Tamari poset $\overline{\mathcal{T}}_3$ with the associated bounded increasing sequences. From definition of $Y_n(k)$ for $k = 1, 2$ and $k = 3$ we have:

$$Y_3(1) = \{((\beta_1), 321), ((\beta_1), 312), ((\beta_1), 231), ((\beta_1), 213), ((\beta_1), 132), ((\beta_1), 123)\} = 6 = 3!$$

$$Y_3(2) = \{((\beta_1, \beta_1), 321), ((\beta_1, \beta_1), 312), ((\beta_1, \beta_1), 231), ((\beta_1, \beta_1), 213), ((\beta_1, \beta_1), 132), ((\beta_1, \beta_1), 123), \\ ((\beta_1, \beta_2), 211), ((\beta_1, \beta_2), 121), ((\beta_1, \beta_2), 112), \\ ((\beta_1, \beta_3), 311), ((\beta_1, \beta_3), 131), ((\beta_1, \beta_3), 113), \\ ((\beta_1, \beta_4), 221), ((\beta_1, \beta_4), 212), ((\beta_1, \beta_4), 122), \\ ((\beta_1, \beta_5), 111)\} = 16 = (3 + 1)^{(3-1)}.$$

$$Y_3(3) = \{((\beta_1, \beta_1, \beta_1), 321), ((\beta_1, \beta_1, \beta_1), 312), ((\beta_1, \beta_1, \beta_1), 231), ((\beta_1, \beta_1, \beta_1), 213), ((\beta_1, \beta_1, \beta_1), 132), \\ ((\beta_1, \beta_1, \beta_1), 123), \\ ((\beta_1, \beta_1, \beta_2), 211), ((\beta_1, \beta_1, \beta_2), 121), ((\beta_1, \beta_1, \beta_2), 112), \\ ((\beta_1, \beta_2, \beta_2), 211), ((\beta_1, \beta_2, \beta_2), 121), ((\beta_1, \beta_2, \beta_2), 112), \\ ((\beta_1, \beta_1, \beta_3), 311), ((\beta_1, \beta_1, \beta_3), 131), ((\beta_1, \beta_1, \beta_3), 113), \\ ((\beta_1, \beta_3, \beta_3), 311), ((\beta_1, \beta_3, \beta_3), 131), ((\beta_1, \beta_3, \beta_3), 113), \\ ((\beta_1, \beta_1, \beta_4), 221), ((\beta_1, \beta_1, \beta_4), 212), ((\beta_1, \beta_1, \beta_4), 122), \\ ((\beta_1, \beta_4, \beta_4), 221), ((\beta_1, \beta_4, \beta_4), 212), ((\beta_1, \beta_4, \beta_4), 122), \\ ((\beta_1, \beta_1, \beta_5), 111), \\ ((\beta_1, \beta_5, \beta_5), 111), \\ ((\beta_1, \beta_2, \beta_3), 311), ((\beta_1, \beta_2, \beta_3), 131), ((\beta_1, \beta_2, \beta_3), 113), \\ ((\beta_1, \beta_2, \beta_5), 111), \\ ((\beta_1, \beta_3, \beta_5), 111), \\ ((\beta_1, \beta_4, \beta_5), 111)\} = 32 = 2^4(4 + 1)^{(4-2)}$$

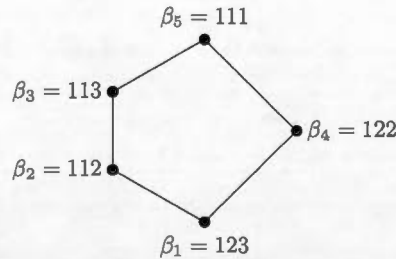


Figure 4.10: The Tamari poset $\overline{\mathcal{T}}_3$ with the associated bounded increasing sequences.

Similarly, by the equation (4.5.1), we have:

$$Y_3(k=1) = \binom{1-1}{1-1} (\#P_{\beta=\beta_1}) = \frac{3!}{1!1!1!} = 6$$

$$\begin{aligned} Y_3(k=2) &= \binom{2-1}{1-1} (\#P_{\beta=\beta_1}) + \binom{2-1}{2-1} (\#P_{\beta=\beta_2} + \#P_{\beta=\beta_3} + \#P_{\beta=\beta_4} + \#P_{\beta=\beta_5}) \\ &= \frac{3!}{1!1!1!} + \left(\frac{3!}{2!1!} + \frac{3!}{2!1!} + \frac{3!}{1!2!} + \frac{3!}{3!} \right) = 16 \end{aligned}$$

$$\begin{aligned} Y_3(k=3) &= \binom{3-1}{1-1} (\#P_{\beta=\beta_1}) + \binom{3-1}{2-1} (\#P_{\beta=\beta_2} + \#P_{\beta=\beta_3} + \#P_{\beta=\beta_4} + \#P_{\beta=\beta_5}) + \binom{3-1}{3-1} (\#P_{\beta=\beta_6} \\ &\quad + \#P_{\beta=\beta_7} + \#P_{\beta=\beta_8} + \#P_{\beta=\beta_9}) \\ &= \frac{3!}{1!1!1!} + 2 \left(\frac{3!}{2!1!} + \frac{3!}{2!1!} + \frac{3!}{1!2!} + \frac{3!}{3!} \right) + \left(\frac{3!}{2!1!} + \frac{3!}{3!} + \frac{3!}{3!} + \frac{3!}{3!} \right) = 32 \end{aligned}$$

So the following results are valid for the zeta polynomial $Y_n(k)$:

- For $k = 1$, we have $Y_n(1) = n!$, which is the number of elements of the set P_{β_1} , where $\beta_1 = \hat{0}$.
- For $k = 2$, we have $Y_n(2) = (n+1)^{(n-1)}$, which is the number of parking functions of length n , associated to the elements of \mathcal{T}_n .
- For $k = 3$, we have $Y_n(3) = 2^n(n+1)^{n-2}$, which is the number of labeled intervals of \mathcal{T}_n .

CHAPTER V

COMBINATORICS OF TUBINGS

In this chapter, we exploit the notion of "tubing" to extend Catalan combinatorics to some classes of simple graphs, showing first that path graphs give back the usual Catalan combinatorics. We consider, two other families of graphs: complete graphs, and cycle graphs. Among the notions that we can thus extend to these two classes of graphs are included the notions of parking functions and Tamari order. After introducing the notion of tubing, we explain how the Catalan "structure" corresponds to "maximal tubing". The conclusion of our story leads to a new notion of parking functions on graphs.

5.1 Tubings of graphs

Informally, a tubing of a graph G is a collection of subsets of the vertices of G that are called tubes. More precisely, as defined in [5], a *tube* is any nonempty subset of the vertices of G whose induced graph is a connected subgraph of G . Two tubes u and v may "interact" as follows:

1. When we have $u_1 \subset u_2$ (with strict inclusion), we say that u_1 is *nested* in u_2 .
2. When we have $u_1 \cap u_2 \neq \emptyset$ and $u_1 \not\subset u_2$ and $u_2 \not\subset u_1$, we say that u and v *intersect*.
3. When we have $u_1 \cap u_2 = \emptyset$ and $u_1 \cup u_2$ is a tube in G , we say that u and v are *adjacent*.

Tubes are said to be *compatible* if they do not intersect, and are not adjacent. When G is connected, a *tubing* U of G is a set of tubes for which every pair of tubes are compatible. A *k-tubing* is a tubing with k tubes. For $S \subset V(G)$, we define the *induced tube* of S , denoted $U|_S$, to be the tube of U that contains S . The *outermost* node of a tube of U is the node that is included in no other smaller tubes of U . For example, Figure 5.1 illustrates valid tubings, and 5.2 illustrates invalid tubings of some connected graphs. In the first graph of Figure 5.1, the red node is the outermost node of the red tube.

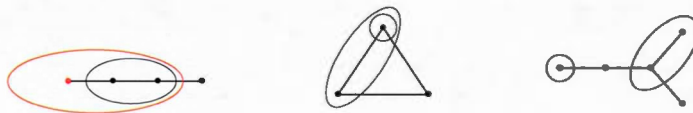


Figure 5.1: Valid tubings of some connected graphs.

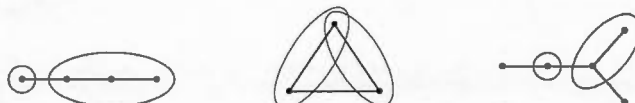


Figure 5.2: Invalid tubings of some connected graphs.

When G has several connected components G_1, \dots, G_k , tubings of G need to satisfy an additional condition. Denoting by u_i the set of vertices of G_i , then any tubing of G can not contain all of the tubes u_i , $1 \leq i \leq k$. We will see that, if G has n vertices, then a tubing of G can contain at most $n - 1$ tubes. For example, Figure 5.3 illustrates valid tubings, and 5.4 illustrates invalid tubings of some graphs with several connected components.



Figure 5.3: Valid tubings of some graphs with several connected components.



Figure 5.4: Invalid tubings of some graphs with several connected components.

For a graph G , the set of tubings of G , which is denoted by $\text{Tub}(G)$, is partially ordered by the relation $U \prec U'$ if U' is obtained from U by adding tubes. For example, Figure 5.5 shows the poset $\text{Tub}(G)$ for a path graph with three nodes. [5, Lemma 2.3.] proves that the geometric realization of the poset $(\text{Tub}(G), \prec)$ is a $(n - 1)$ -dimensional polytope whose vertices are indexed by $(n - 1)$ -tubings, and edges by $(n - 2)$ -tubings of G .

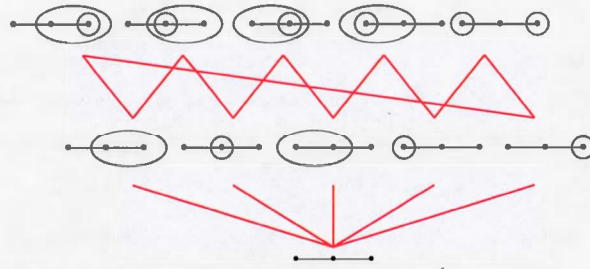


Figure 5.5: Poset of tubings of a path graph with 3 nodes.

Maximal tubing

For a graph G with n vertices, we denote by M_G the set of *maximal tubings* of G . As shown in [7], maximal tubings in $\text{Tub}(G)$ are precisely those that contain $n - 1$ tubes. Thus, $n - 1$ vertices of G are contained in tubes except one vertex that we call *untubed*. For example, the top row of Figure 5.5 corresponds to the set of maximal tubings of a 3-vertex path graph which has five elements. Here is some observations about a maximal tubing $U \in M_G$.

- There is a unique untubed vertex, denoted r .
- All other vertices belong to some tubes.

For path graphs there are special further properties:

- The vertex r naturally separates the set of other vertices of the path graph into two portions. We define L and R respectively to be the set of vertices on the left and right of r .
- No tube contains both $x \in L$ and $y \in R$ (if there exists such tube, it should contain r , and this is a contradiction).
- By the definition of induced tube, $U|_L$ (resp. $U|_R$) is a tube (if not, U is not maximal).

The cardinality of the set of maximal tubings of n -vertices path graphs is equal to $C(n) = \frac{1}{n+1} \binom{2n}{n}$. Hence, there is a bijection between maximal tubings of a path graph and Catalan objects. As we will see in the next section, this bijection is very natural.

5.2 Path graphs give Catalan objects

Path graphs are interesting for us because of the cardinality of their maximal tubings. The maximal tubings of a n -path graph is another Catalan object. As before, we study the Tamari order and parking functions in terms of them. This will prepare the ground for our generalization of the notion of parking functions to graphs.

5.2.1 Bijection between maximal tubings of path graph and binary trees

We already know about various families of Catalan objects (see Chapter 2), and how these are bijectively related to one another. Here we relate maximal tubings to one of these families: binary trees. Our bijection $f : M_G \rightarrow B_n$, is recursively constructed as follows.

For a given maximal tubing U of the n -path graph, its untubed vertex r , is going to become the root of the associated binary tree. As explained before, $U|_L$ and $U|_R$ are both tubes. Then, $f(U)$ is a binary tree with root r , and left (resp. right) branch $f(U|_L)$ (resp. $f(U|_R)$). Figure 5.6, illustrates the function f in general.

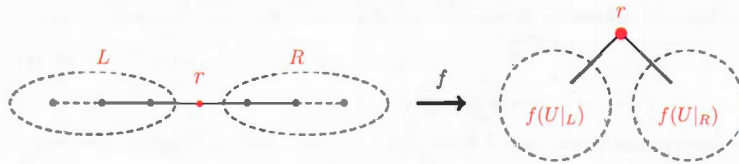
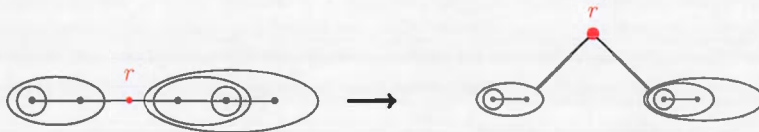


Figure 5.6: Representation of function f .

We repeat this process for the left (resp. right) sub-path graph inside $U|_L$ (resp. $U|_R$), whose tubes are those of U containing only vertices in L (resp. R), except L (resp. R) itself, until reaching the smallest tubes which contain just one node of the path graph. For example, associating a maximal tubing of the 6-path graph to a binary tree of size six, is illustrated in Figure 5.7.



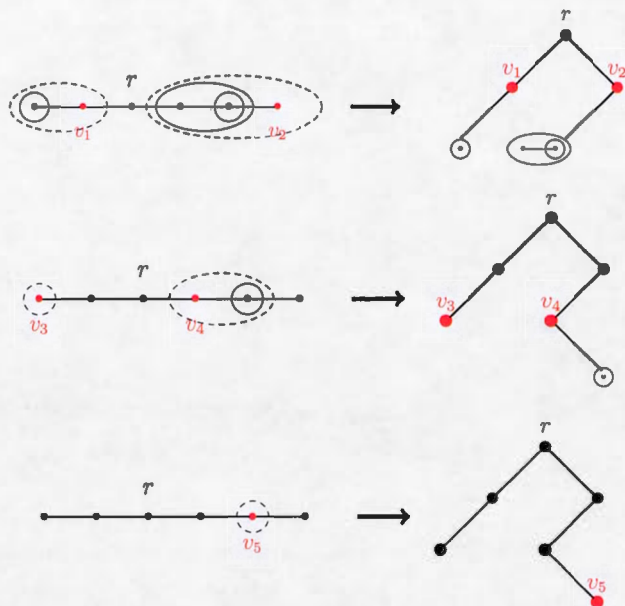
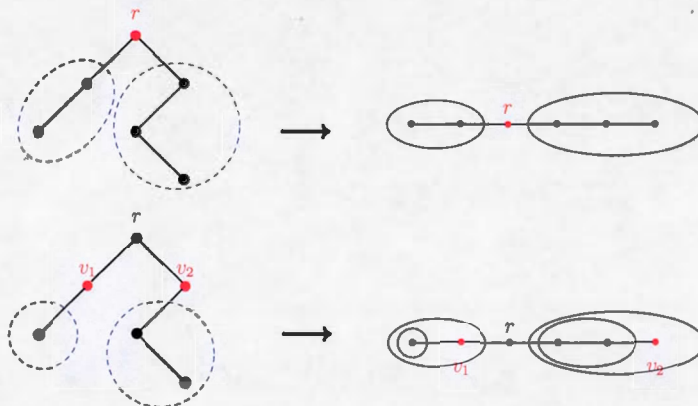


Figure 5.7: Transforming a maximal tubing of a path graph to the corresponding binary tree.

To describe the inverse of function f , we denote by τ the root of a given binary tree with n nodes. This is going to become the untubed vertex of the associated n -path graph. Denote by $T|_L$ the left subtree (resp. by $T|_R$ the right subtree). Hence, $f^{-1}(T|_L)$ is L , which is the set of vertices of the path graph in the left side of vertex τ (resp. $f^{-1}(T|_R)$ is R). We denote by $U|_L$ the induced tube that contains vertices of L (resp. $U|_R$ contains vertices of R), and repeat this process for the left (resp. right) subtree until reaching the vertices of the tree without any children. For example, Figure 5.8 illustrates associating a binary tree with six nodes to a maximal tubing of 6-path graph.



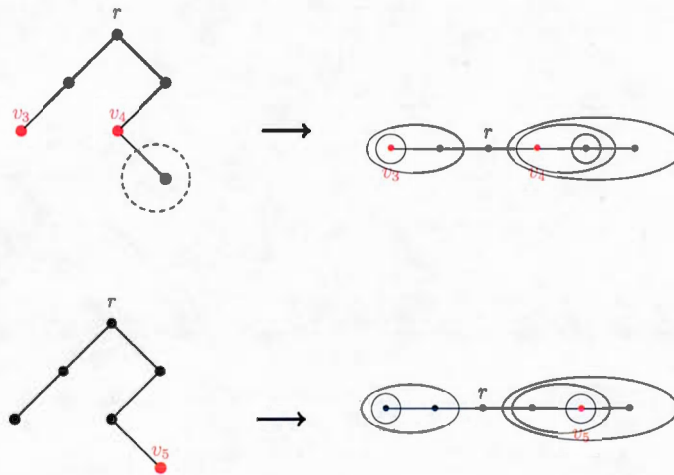


Figure 5.8: Transforming a binary tree to the corresponding maximal tubing of a path graph.

5.2.2 Tamari order on maximal tubings of path graphs

Let G be a path graph with n vertices labeled $\{1, \dots, n\}$ so that $\{i, i + 1\}$ is an edge. As defined in [8], for two $(n - 1)$ -tubings U_1, U_2 of $(\text{Tub}(G), \prec)$, we say that U_2 covers U_1 if they have all the same tubes except for one differing pair such that the label of outermost vertex on that pair, is greater for U_2 . To compare U_1 and U_2 we can also write down the sets of vertices in each tube, and then the differing pair would appear in these sets. For example, Figure 5.9 illustrates a covering relation between two maximal tubings of the path graph with four vertices labeled 1, 2, 3, and 4 respectively. The differing pair is specified in red. The label of the outermost node in U_1 is 2 and in U_2 is 4 so $U_1 \prec U_2$.

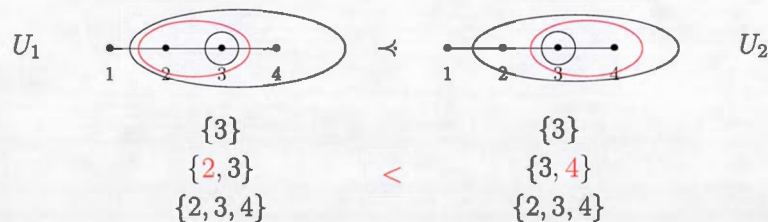


Figure 5.9: Notion of $U_1 \prec U_2$.

The set of maximal tubings of G with the mentioned Tamari order, is in fact a lattice [7, 8]. For example, Figure 5.10 represents the Tamari lattice of maximal tubings of G with $n = 3$ and $n = 4$ vertices. By removing the differing tubes between the pairs (U_1, U_2) such that $U_1 \prec U_2$, we have $(n - 2)$ -tubings that correspond to the edges of the Hasse diagram of the Tamari lattice.

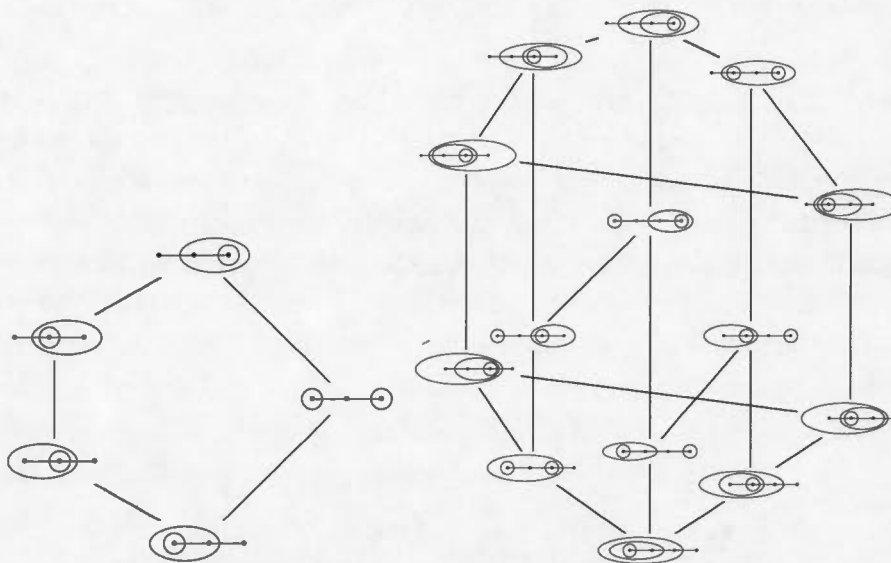


Figure 5.10: The Tamari lattice that results from maximal tubings on the path graph for $n=3$ (left) and $n=4$ (right).

In another simpler view, the Tamari order on the set of maximal tubings of a path graph with n vertices, is given by pushing the tubes by rightward applications of the associative law $(xy)z = x(yz)$. Hence let U_1 and U_2 be two tubings of a path graph then, U_2 covers U_1 , if U_2 is obtained from U_1 by pushing the tubes in order from smallest, left to the right, so that the compatibility condition is preserved. Note that because of keeping the compatibility on tubes of a tubing, maybe we have to change the size of the tubes (i.e. the number of vertices that the tube contains) during the pushing. For example, in Figure 5.11 the red small tube during the pushing left to right, has to be bigger to keep the compatibility.



Figure 5.11: Pushing the tubes in order from smallest one, right to left.

5.2.3 Parking functions on maximal tubings of path graphs

As mentioned in Chapter 4, one of our interests is the notion of parking functions on Catalan objects, so here we want to study parking functions on the set of maximal tubings of a path graph with n vertices. To associate a parking function to a $(n - 1)$ -tubing of the n -path graph, we first need to define compatible labeling.

For a maximal tubing of a n -path graph, vertices labeled $\{1, \dots, n\}$ so that $\{i, i + 1\}$ is an edge, a *compatible labeling* is defined as follows. We put labels $\{1, 2, \dots, n\}$ on the vertices, starting from the first vertex, and moving along the path until the n -th vertex. The positions of tubes (for putting the red labels) are important because, each time that we enter a tube, the label must decrease. For example, Figure 5.12 illustrates a compatible labeling of a maximal tubing of a 5-path graph.

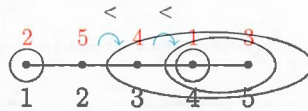
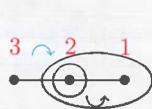


Figure 5.12: A compatible labeling for a path graph with five vertices.

Proposition. There is a bijection between the compatible labeling of maximal tubings of a n -path graph and parking functions.

Proof. For each compatible labeling of a path graph, we can get parking function f by setting $f(x) = i + 1$ if and only if label x occurs after i -times exiting from the left previous tubes. For example, for the maximal tubing of Figure 5.13 (which is bijectively equal to the binary tree of Figure 4.8) there are exactly three compatible labeling, so we have three parking functions associated with this maximal tubing of 3-path graph.



$$f(3) = 1$$

$$f(2) = 1$$

$$f(1) = 2$$



211 is a parking function.

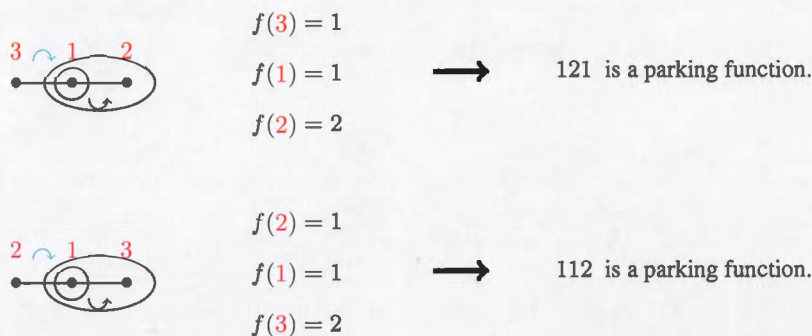


Figure 5.13: Parking functions on the maximal tubing of a 3-path graph.

Furthermore, for a given parking function, obtaining the labeled maximal tubing of path graph is possible by using introduced bijection in Chapter 2 and 5.2.1.

5.3 Maximal tubings of other special families of graphs

In this section we want to study the set of maximal tubings for other families of graphs and count the number of such maximal tubings for each of the families. Also we want to find a covering relation between the elements of M_G for each of the families to help us study about their lattice (see [8] for more details, and figures in dimension four).

5.3.1 Complete graphs

Let G be the complete graph with n vertices. Each maximal tubing of G can be seen as a sequential nesting of all n vertices. Hence the set M_G contains $n!$ tubes. Therefore, there is a bijection between maximal tubings of a complete graph with n vertices labeled $\{1, 2, \dots, n\}$, and permutations of $\{1, 2, \dots, n\}$. A permutation σ corresponds to a maximal tubing that the tubes are

$$\{\sigma^{-1}(1)\}, \{\sigma^{-1}(1), \sigma^{-1}(2)\}, \dots, \{\sigma^{-1}(1), \sigma^{-1}(2), \dots, \sigma^{-1}(n-1)\}$$

respectively from the smallest, and $\{\sigma^{-1}(n)\}$ is not in a tube. Furthermore, a maximal tubing of G gives a permutation of \mathbb{S}_n where the vertices are inputs for the permutation and the output is the relative tube size. Hence, weak order on permutations and Tamari order of Section 5.2.2 can be generalized to maximal tubings of the complete graph with vertices labeled by $\{1, 2, \dots, n\}$. For example, Figure

5.14 shows a covering relation between two maximal tubings of the complete graph with three vertices labeled with 1, 2, 3, and their corresponding permutations.

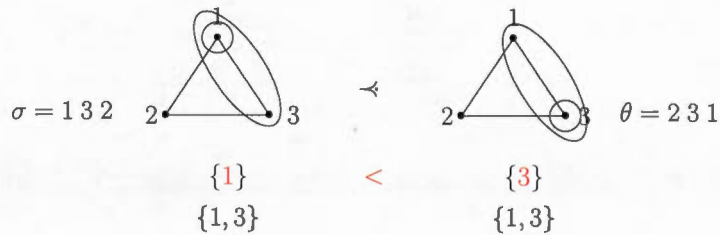


Figure 5.14: A covering relation in the weak order on permutations.

The Hasse diagram of the lattice that results from tubings of a complete graph with n vertices is combinatorially equivalent to the 1-skeleton of the "permutahedron", as explained in [8]. For example, Figure 5.15 shows the lattice that results from maximal tubings on the complete graph with 3 vertices.

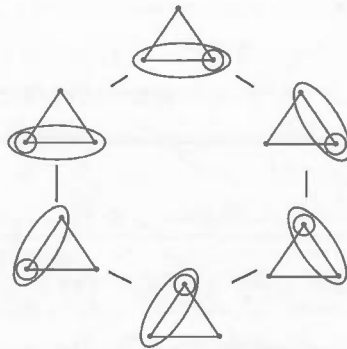


Figure 5.15: The lattice that results from maximal tubings on the complete graph with 3 vertices.

5.3.2 Discrete graphs

Let G be the discrete graph on n nodes labeled $\{1, \dots, n\}$ so that $(i + 1)$ -th node is placed after i -th one. each maximal tubing of G according to the definition of tubing of a graph with several connected com-

ponents is choosing $n - 1$ out of n possible nodes. Hence the set M_G has n elements. The same covering relation as what we defined in Section 5.2.2, or pushing the tubes right to left that preserve compatibility, gives the lattice on maximal tubings of n -disjoint nodes. For example, Figure 5.16 illustrates the lattice that results from maximal tubings of three disjoint nodes.

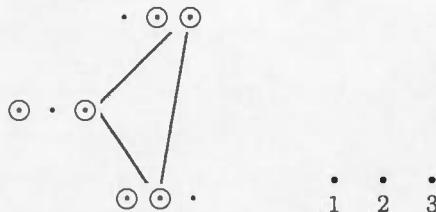


Figure 5.16: The lattice that results from maximal tubings on the three disjoint nodes.

In [7], the Hasse diagram of the lattice that results from maximal tubings of the n - disjoint nodes, is recovering the 1-skeleton of the "simplex" with dimension $n - 1$.

5.3.3 Cycle graphs

As discussed in [7], there are $\binom{2(n-1)}{n-1}$ maximal tubings for a cycle graph with n vertices. Some of the maximal tubings of a cycle graph are seen as a sequential nesting of all vertices, and the rest of them are other compatible cases. The same covering relation as what we defined in Section 5.2.2, gives the lattice on maximal tubings of the cycle graph with n vertices. This lattice is combinatorially equivalent to the 1-skeleton of the "cyclohedron" (see [8]). For example, Figure 5.15 similarly, is a lattice that results from the cycle graph with 3 vertices.

5.3.4 Star graphs

There are $\sum_{k=0}^n \frac{n!}{k!}$ maximal tubings for a star graph S_n (a tree with one internal node and n leaves). One of the maximal tubings of a star graph is tubing all the leaves by the smallest size of tubes, and in the others, the bigger size of tubes contain both the internal node and $n - 1$ leaves, in all compatible cases. The same covering relation as what we defined in Section 5.2.2, gives the lattice on maximal tubings of the star graph S_n so that $(n - 1)$ vertices as leaves labeled by $\{1, \dots, (n - 1)\}$ respectively, and internal

vertex labeled by n . This lattice is combinatorially equivalent to the 1-skeleton of the "stellohedron" (see [8]). For example, Figure 5.17 shows the lattice that results from maximal tubings on the star graph S_2 .

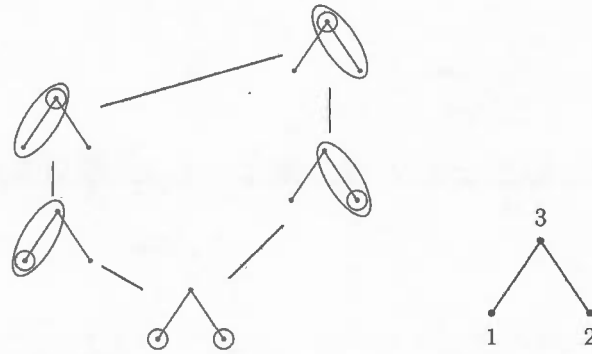


Figure 5.17: The lattice that results from maximal tubings on the star graph S_2 .

5.4 Toward a new generalization of parking functions to graphs

A compatible labeling for a maximal tubing of other special families of graphs is as follows. We are forced to label the vertices, starting with the untubed vertex, and following the tubes from the biggest to the smallest. Each time that we enter a tube, the label must decrease. For example, Figure 5.18 illustrates a compatible labeling of a maximal tubing of a cycle graph with three vertices.

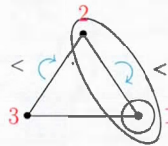


Figure 5.18: A compatible labeling for a cycle graph with three vertices.

The special case of compatible labeling in Section 5.2.3, yield us to a parking functions on maximal tubings of path graphs, and our aim is doning the same for other families of graphs.

CONCLUSION

We have seen that the notion of tubing allows for the generalization of Catalan structures, Tamari posets, and parking functions to other classes of graphs, with path graphs corresponding to the classical setup. In the process of doing so, we have observed that:

- Parking functions for complete graphs are easy to enumerate, since each maximal tubing of a complete graph is a sequential nesting of all vertices, therefore for each maximal tubing of G , there is just one compatible labeling. The total number of these labelings is $n!$. For example, Figure 5.19 illustrates six compatible labelings on maximal tubings of the complete graph with three vertices.

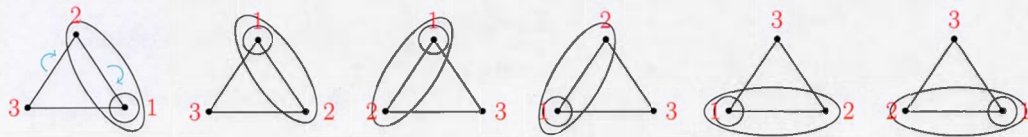


Figure 5.19: Compatible labelings on maximal tubings of the complete graph with three vertices.

- For cycle graphs, and star graphs, we follow the same compatible labeling such as complete graphs. The difference is that, for some of the maximal tubings of these graphs there is more than one such labeling. For a graph G with n vertices, Table 5.1 for cycle graphs, and Table 5.2 for star graphs, represent what we have guessed for small values of n .

To extend some of the topics discussed in this work to maximal tubings of other "nice" families of graphs, some questions to consider are:

1. Find a formula for the number of maximal tubings for other "nice" families of graphs.
2. Find the structure of the poset of maximal tubings for other "nice" families of graphs, and an explicit description of the relevant poset.

3. Find the number of compatible labelings of maximal tubings for other "nice" families of graphs.
4. Calculate the zeta polynomial for the poset of maximal tubings of these other families.

n	$\#M_G$	$\#\text{labelings of } M_G$
3	6	6
4	20	24
5	70	120
	$\binom{2(n-1)}{n-1}$?

Table 5.1: Some values of maximal tubings and compatible labelings of maximal tubings for cycle graphs.

n	$\#M_G$	$\#\text{labelings of } M_G$
2	5	6
3	16	24
4	65	120
	$\sum_{k=0}^n \frac{n!}{k!}$?

Table 5.2: Some values of maximal tubings and compatible labelings of maximal tubings for star graphs.

Lots of other questions could also be considered, taking into account the extensive work of

- M. Carr and S. Devadoss in [5, 2005], and Devadoss continued in [7, 2007].
- M. Ronco [11, 2012].
- S. Forcey in [8, 2012].

BIBLIOGRAPHY

- [1] D. Armstrong, N. A. Loehr, and G. S. Warrington. Rational parking functions and catalan numbers. *arXiv:1403.1845v1*, 2014.
- [2] M. Beck, A. Berrizbeitia, M. Dairyko, C. Rodriguez, A. Ruiz, and S. Veeneman. Parking function, shi arrangements, and mixed graphs. *arXiv:math/1405.5587v2*, 2014.
- [3] F. Bergeron, P. Leroux, and G. Labelle. Combinatorial species and tree-like structures. *Encyclopedia of Mathematics, Cambridge University Press*, 1998. 497, 1998.
- [4] M. Bousquet-Mélou, G. Chapuy, and L. F. Préville-Ratelle. The representation of the symmetric group on m -tamari intervals. *Electron. J. Combin.*, *arXiv:1202.5925v3*, 2013.
- [5] M. Carr and S. Devadoss. Coxeter complexes and graph associahedra. *Topology and its Appl.* 153, pages 2155–2168, 2006.
- [6] F. Chapoton. Sur le nombre d'intervalles dans les treillis de tamari. *Sém. Lothar. Combin.* 55, 2006.
- [7] Satyan L. Devadoss. A realization of graph-associahedra. *Discrete Math.*, 309, 2009.
- [8] Stefan Forcey. Extending the tamari lattice to some compositions of species. *Associahedra, Tamari lattices and related structures, volume 299, pages 187-210. Springer Basel*, 2012.
- [9] A.G. Konheim and B. Weiss. An occupancy discipline and applications. *SIAM J. Appl. Math.* 14, 1266-1274, 1966.
- [10] F. Müller-Hoissen, J. Pallo, J. Marcel, and J. Stasheff (Eds.). Associahedra, tamari lattices and related structures: Tamari memorial festschrift., *Progress in Mathematics, Vol. 299*, 2012.
- [11] M. Ronco. Generalized tamari order. *Associahedra, Tamari Lattices, and Related Structures, Volume 299, pages 339-350. Springer Basel*, 2012.
- [12] R. P. Stanley. Enumerative combinatorics. *Cambridge University Press, Cambridge*, Vol. 1, 1997.
- [13] R. P. Stanley. Enumerative combinatorics. *Cambridge University Press, Cambridge*, Vol. 2, 2001.
- [14] D. Tamari. Monoïdes préordonnés et chaînes de nalcev. *Thèse de doctorat, Université de Paris*, 1951.
- [15] D. Tamari. The algebra of bracketings and their enumeration. *Nieuw Archief voor Wiskunde, Ser. 3 10: 131-146*, 1962.
- [16] Lauren K. Williams. Cluster algebras: An introduction. *arXiv:math/1212.6263v3*, 2013.

INDEX

- B_n , see binary trees 13
- $C(n)$, see Catalan numbers 10
- C_n , see complete binary trees 14
- D_n , see Dyck paths 14
- M_G , see maximal tubings of G 45
- P_n , see parking functions 32
- $Z_P(n)$, see zeta polynomials 8
- S_n , see symmetric group 10
- B_n , see bounded increasing sequences 19
- T_n , see Tamari lattice 23
- $\text{Tub}(G)$, see tubings of G 44
- \prec , see covering relation 5
- bounded increasing sequences, 19, 33
- Catalan numbers, 10
- chain, 5
 - multi-chain, 5
- compatible labeling, 50
- covering relation, 5
- Dyck path, 14
 - labeled, 34
- Dyck word, 16
- graph, 3
 - complete, 5
 - connected, 4
 - components, 4
 - cycle, 5
 - path, 4
 - star, 54
 - subgraph, 4
 - induced, 4
- Hasse diagram, 5
- interval, 6
 - labeled, 37
- lattice, 9
 - Tamari, 23, 48
- parking function, 32, 50
- poset, 5
 - comparable and incomparable elements, 5
 - maximal and minimal elements, 5
 - maximum and minimum elements, 5
- post order, 17, 40
- rotation operation, 25
- symmetric group, 10
 - cycle decomposition, 11
- tree, 13
 - binary, 13
 - complete binary, 14
 - root, 13
 - size, 13
- tube, 43
 - adjacent, 43
 - compatible, 43
 - induced, 43
 - intersect, 43
 - nested, 43
 - untubed, 45
- tubing, 43
 - k -tubing, 43
 - maximal, 45
- vertical run, 14
- weak order, 11
- Young subgroup, 11, 33
- zeta polynomial, 8, 41